



## Original article

# Small molecule deoxyxyboquinone triggers alkylation and ubiquitination of Keap1 at Cys489 on Kelch domain for Nrf2 activation and inflammatory therapy

Ke-Gang Linghu<sup>a, d, 1</sup>, Tian Zhang<sup>a, 1</sup>, Guang-Tao Zhang<sup>c</sup>, Peng Lv<sup>a</sup>, Wen-Jun Zhang<sup>c</sup>, Guan-Ding Zhao<sup>a</sup>, Shi-Hang Xiong<sup>a</sup>, Qiu-Shuo Ma<sup>a</sup>, Ming-Ming Zhao<sup>a</sup>, Meiwan Chen<sup>a</sup>, Yuan-Jia Hu<sup>a</sup>, Chang-Sheng Zhang<sup>c, \*\*</sup>, Hua Yu<sup>a, b, \*</sup>

<sup>a</sup> State Key Laboratory of Quality Research in Chinese Medicine, Institute of Chinese Medical Sciences, University of Macau, Macao SAR, China

<sup>b</sup> Macao Centre for Research and Development in Chinese Medicine, Institute of Chinese Medical Sciences, University of Macau, Macao SAR, China

<sup>c</sup> Key Laboratory of Tropical Marine Bio-resources and Ecology, Guangdong Key Laboratory of Marine Materia Medica, RNAM Center for Marine Microbiology, South China Sea Institute of Oceanology, Chinese Academy of Sciences, Guangzhou, 510301, China

<sup>d</sup> State Key Laboratory of Functions and Applications of Medicinal Plants & School of Pharmaceutical Sciences, Guizhou Medical University, Guiyang, 550025, China

## ARTICLE INFO

## Article history:

Received 18 April 2023

Received in revised form

13 July 2023

Accepted 13 July 2023

Available online 17 July 2023

## Keywords:

Deoxyxyboquinone

Anti-inflammation

Target

Keap1/Nrf2

Alkylation

Ubiquitination

## ABSTRACT

Activation of nuclear factor erythroid 2-related factor 2 (Nrf2) by Kelch-like ECH-associated protein 1 (Keap1) alkylation plays a central role in anti-inflammatory therapy. However, activators of Nrf2 through alkylation of Keap1-Kelch domain have not been identified. Deoxyxyboquinone (DNQ) is a natural small molecule discovered from marine actinomycetes. The current study was designed to investigate the anti-inflammatory effects and molecular mechanisms of DNQ via alkylation of Keap1. DNQ exhibited significant anti-inflammatory properties both *in vitro* and *in vivo*. The pharmacophore responsible for the anti-inflammatory properties of DNQ was determined to be the  $\alpha$ ,  $\beta$ -unsaturated amides moieties by a chemical reaction between DNQ and *N*-acetylcysteine. DNQ exerted anti-inflammatory effects through activation of Nrf2/ARE pathway. Keap1 was demonstrated to be the direct target of DNQ and bound with DNQ through conjugate addition reaction involving alkylation. The specific alkylation site of DNQ on Keap1 for Nrf2 activation was elucidated with a synthesized probe in conjunction with liquid chromatography-tandem mass spectrometry. DNQ triggered the ubiquitination and subsequent degradation of Keap1 by alkylation of the cysteine residue 489 (Cys489) on Keap1-Kelch domain, ultimately enabling the activation of Nrf2. Our findings revealed that DNQ exhibited potent anti-inflammatory capacity through  $\alpha$ ,  $\beta$ -unsaturated amides moieties active group which specifically activated Nrf2 signal pathway via alkylation/ubiquitination of Keap1-Kelch domain, suggesting the potential values of targeting Cys489 on Keap1-Kelch domain by DNQ-like small molecules in inflammatory therapies.

© 2023 The Authors. Published by Elsevier B.V. on behalf of Xi'an Jiaotong University. This is an open access article under the CC BY-NC-ND license (<http://creativecommons.org/licenses/by-nc-nd/4.0/>).

## 1. Introduction

Inflammatory and oxidative damages are prevalent pathological mechanisms that initiate a range of acute and chronic illnesses. The

interplay between these processes exacerbates the progression of the disease [1,2]. The human body has developed various defense mechanisms to counteract cellular damage caused by oxidative stress and inflammation [3]. Kelch-like ECH-associated protein 1 (Keap1)-nuclear factor erythroid 2-related factor 2 (Nrf2)-antioxidant response elements (ARE) pathway represents one of the most important cellular defense mechanisms against oxidative stress and safeguard various organs and cells from xenobiotic harm [4]. The activation of Keap1/Nrf2/ARE has been extensively demonstrated to produce a protective function in various diseases, including atherosclerosis, multiple sclerosis, Parkinson's disease, Alzheimer's disease, inflammatory bowel disease, and rheumatoid arthritis [5,6]. Therefore, targeting to Keap1-Nrf2-ARE signaling pathway has been

Peer review under responsibility of Xi'an Jiaotong University.

\* Corresponding author. State Key Laboratory of Quality Research in Chinese Medicine, Institute of Chinese Medical Sciences, University of Macau, Macao SAR, China.

\*\* Corresponding author.

E-mail addresses: [czhang@scsio.ac.cn](mailto:czhang@scsio.ac.cn) (C.-S. Zhang), [bcaley@um.edu.mo](mailto:bcaley@um.edu.mo) (H. Yu).

<sup>1</sup> Both authors contributed equally to this work.

<https://doi.org/10.1016/j.jpha.2023.07.009>

2095-1779/© 2023 The Authors. Published by Elsevier B.V. on behalf of Xi'an Jiaotong University. This is an open access article under the CC BY-NC-ND license (<http://creativecommons.org/licenses/by-nc-nd/4.0/>).

deemed a logical approach for identifying potential therapeutic agents in the treatment of inflammatory disorders [7].

Keap1 is a cysteine-rich cytoplasmic protein that functions as a negative regulator of Nrf2. There are totally 27 cysteine residues located in five domains of Keap1 including NTR, BTB, IVR, Kelch (DGR) and CTR [8,9]. In a state of basal activity, Nrf2 forms a bond with the Keap1-Kelch domain and undergoes continuous ubiquitination by the Keap1-Cul3-Ligase complex, ultimately resulting in degradation of Nrf2 within the 26S proteasome [5,10]. Upon cellular exposure to electrophiles or oxidative stress, Nrf2 could evade Keap1-mediated ubiquitination and subsequent degradation. Subsequently, Nrf2 translocates to the nucleus and binds with ARE to initiate the expression of antioxidative and anti-inflammatory proteins, such as heme oxygenase 1 (HO-1), NAD(P)H:quinine oxidoreductase (NQO1), and glutamate cysteine ligase (GCL) [6,11]. It has been observed that the activation of Nrf2-dependent transcription of anti-inflammatory proteins through electrophiles is facilitated by the alkylation of Keap1 cysteine residues [11]. However, activators of Nrf2 through alkylation at Keap1-Kelch domain in inflammatory treatment remains elusive.

Deoxyxyloquinone (DNQ, Fig. S1A), a diazaanthraquinone compound with the molecular formula of  $C_{15}H_{12}N_2O_4$  ( $m/z$  284.08), was firstly reported in 1961 [12] and established a synthetic route by Bair et al. [13] in 2010. Zhang and the co-workers [14] discovered the natural DNQ from marine actinomycetes and confirmed the structure by X-ray crystallographic analysis in 2011, and constructed a massively bio-synthesized route with a deep-sea aerobic actinomycete (*Pseudonocardia antitumoralis* sp. nov.) [15]. Previously, DNQ was reported to exhibit great potentials in cancer chemotherapy via specifically targeting to cancer cells [16] in a distinguished mechanism with other therapeutic agents like metal-based drugs [17–19], traditional medicine [20], polymeric nanomedicines [21] and others [22,23]. Interestingly, Bair et al. [13] identified that DNQ upregulated *Hmox1* gene expression (the Top 1 upregulated gene) in U-937 human myeloid leukaemia cells. HO-1 protein (encoded by the *Hmox1* gene) is an anti-inflammatory marker widely reported in the anti-inflammatory process of small molecules [11]. However, the anti-inflammatory activity of DNQ is unclear. In this study, we demonstrated the anti-inflammatory effects of DNQ in various cell lines and lipopolysaccharide-induced acute inflammatory mice via upregulating anti-inflammatory genes including *Hmox1* gene, which was at least involved in regulating Keap1/Nrf2 signaling pathway through direct alkylation of Keap1-Kelch domain.

## 2. Materials and methods

### 2.1. Chemicals and reagents

Tris (2-carboxyethyl) phosphine hydrochloride (TCEP), 3-[4, 5-dimethyl-2-thiazolyl]-2, 5-diphenyltetrazolium bromide (MTT), lipopolysaccharides (LPS, *Escherichia coli* O111:B4), dimethyl sulfoxide (DMSO), dimethyl fumarate (DMF), glutathione (GSH), *N*-acetylcysteine (NAC), Anti-FLAG<sup>®</sup> M2 magnetic beads, (R)-MG132, phorbol 12-myristate 13-acetate (PMA), Griess reagent, DL-dithiothreitol (DTT), iodoacetamide (IAA), formic acid (FA), acetonitrile (ACN), methanol, and biotin-dPEG<sup>®</sup>3-MAL were purchased from Sigma-Aldrich (St. Louis, MO, USA). 4',6-diamidino-2-phenylindole (DAPI), dichlorodihydrofluorescein diacetate (DCFH-DA) and radioimmunoprecipitation assay (RIPA) lysis buffer were obtained from Beyotime Institute of Biotechnology (Nantong, China). 3-(but-3-yn-1-yl)-3-(2-iodoethyl)-3H-diazirine, biotin-PEG3-azide and tris (benzyltriazolylmethyl) amine (TBTA) were purchased from GreenChem (Taizhou, China).

The acquisition of protein A/G PLUS-agarose was from Santa Cruz Biotechnology (Dallas, Texas, USA). Pierce<sup>™</sup> BCA protein assay

kit, TRIzol<sup>™</sup> reagent, Pierce<sup>™</sup> monomeric avidin agarose, Pierce<sup>™</sup> anti-c-Myc magnetic beads, lipofectamine<sup>™</sup> 3,000 transfection reagent, and opti-MEM<sup>™</sup> I reduced serum medium, fetal bovine serum (FBS), 0.25% trypsin-EDTA ( $m/v$ ), Dulbecco's modified Eagle's medium (DMEM), penicillin-streptomycin (10,000 U/mL, P/S), and phosphate-buffered saline (PBS), phenylmethylsulfonyl fluoride (PMSF) and protease inhibitor cocktail were purchased from Thermo Fisher Scientific (Waltham, MA, USA). Trypsin/chymotrypsin (MS grade) were purchased from Promega (Madison, WI, USA). Enzyme-linked immunosorbent assay (ELISA) kits were supplied by Neobioscience Technology Co., Ltd. (Shenzhen, China). Primary antibodies against iNOS (#13120; 1:1000), NLRP3 (#15101; 1:1000), Myc-Tag (#2276; 1:1000), Calreticulin (D3E6) XP<sup>®</sup> Rabbit mAb (Alexa Fluor<sup>®</sup> 594 Conjugate) (#77344; 1:50) and the secondary antibody (#7076, #7074; 1:2000) were purchased from Cell Signaling Technology (Danvers, MA, USA). Primary antibodies against HO-1 (#10701-1-AP; 1:1000), GCLM (#14241-1-AP; 1:2000), KEAP1 (#10503-2-AP; 1:2000), NRF2 (#16396-1-AP; 1:2000), Ubiquitin (#10201-2-AP; 1:500) and Flag tag (#66008-4-Ig; 1:5000) were purchased from Proteintech (Rosemont, IL, USA).  $\beta$ -actin (#CPA1009; 1:1000) was purchased from Cohesion Biosciences (Suzhou, China). Recombinant human KEAP1 protein (His & GST Tag) was purchased from Sino Biological (Beijing, China). NATE<sup>™</sup> nucleic acid transfection enhancer was obtained from InvivoGen (San Diego, CA, USA).

### 2.2. Cell culture

All cells were cultured in indicated media at 37 °C in an atmosphere of 95% humidity and 5% CO<sub>2</sub>. Human THP-1 monocytes, U-937, and A549 cells were cultured in RPMI-1640 medium containing 10% FBS and 1% P/S. THP-1 monocytes were differentiated into macrophages by 24 h incubation with 50 ng/mL PMA followed by 48 h incubation in RPMI-1640 medium containing 10% FBS and 1% P/S. Human embryonic kidney 293T (HEK293T), mouse BV2 microglial cells and mouse monocyte macrophage RAW264.7 cells were cultured in DMEM supplemented with 10% FBS and 1% P/S. Mouse AML12 cells were cultured in DMEM/F12 containing 10% FBS and 1% P/S. All cell lines were obtained from American Type Culture Collection (Manassas, VA, USA).

### 2.3. Cell viability measurement

The assessment of cell viability was conducted via the utilization of the MTT assay, employing previously established methods [24]. In brief, the cells were cultured in a 96-well plate and allowed to adhere overnight. Subsequently, the cells were treated with DNQ at specified concentrations for 12 h. Thereafter, the cells were subjected to incubation with a fresh medium that contained 0.5 mg/mL MTT for an additional 3 h. The liquid portion of the sample was extracted and the optical density of the formazan dye that had been dissolved in 150  $\mu$ L of DMSO was measured at a wavelength of 490 nm using the FlexStation 3 microplate reader (Molecular Devices, San Jose, CA, USA).

### 2.4. Lactate dehydrogenase (LDH) assay

The LDH assay in the cell culture medium was conducted with a LDH cytotoxicity assay kit (#88953; Thermo Fisher Scientific) following the manufacturer's instruction.

### 2.5. Nitric oxide (NO) assay

BV2 and RAW264.7 cells were treated with the indicated concentrations of DNQ for 1 h, followed by stimulation with LPS for

12 h. No content in the supernatant was determined using the Griess reagent according to the manufacturer's protocol.

### 2.6. Intracellular reactive oxygen species (ROS) detection

RAW264.7 cells were treated with the indicated concentrations of DNQ for 1 h, followed by stimulation with LPS for 12 h. Intracellular ROS was probed with the DCFH-DA according to the manufacturer's protocol, subsequently detected with a flow cytometer (Becton Dickinson, San Jose, CA, USA).

### 2.7. Immunofluorescence staining

The immunofluorescence staining methods, as previously reported [25], were utilized to detect the nucleus expression of Nrf2 in RAW264.7 and BV2 cells. In brief, the cells were seeded into a confocal culture dish and left overnight. Following a 6 h treatment with DNQ, the cells underwent a single wash with PBS and were subsequently fixed with 4% paraformaldehyde for 10 min. The cells were then washed with a washing solution and blocked with 3% bovine serum albumin (BSA). Following this, the cells underwent incubation with Nrf2 antibody for 1 h. Subsequently, the cells were subjected to three washes with a washing solution, after which they were incubated with a fluorescent secondary antibody for 1 h. Subsequently, the cells were subjected to staining with DAPI for 4 min, and finally, visualized using a confocal laser microscope (Leica, Buffalo Grove, IL, USA).

### 2.8. ELISA

The contents of cytokines in cell culture medium and mice serum were determined with the ELISA kits according to the manufacturer's protocol.

### 2.9. Western blot

The expressions of indicated proteins were detected by Western blot with the methods previously reported [25]. In summary, the protein was extracted from the collected cells utilizing RIPA lysis buffer and its quantification was performed through employment of a BCA protein assay kit. The protein samples, ranging from 15 to 40  $\mu\text{g}$ , underwent separation via sodium dodecyl sulphate-polyacrylamide gel electrophoresis (SDS-PAGE) with either an 8% or 10% concentration. Following separation, the proteins were transferred to a polyvinylidene fluoride membrane. The membrane underwent a blocking process utilizing 5% defatted dry milk for a duration of 2 h. Following this, it was subjected to an overnight incubation at 4 °C with primary antibodies. After washing, the membrane was incubated with the secondary antibody for 1.5 h at room temperature. The visualization of the blot was achieved through the utilization of an enhanced chemiluminescence kit (GE Healthcare, Buckinghamshire, UK).

### 2.10. Quantitative polymerase chain reaction (qPCR)

The extraction of total RNA from the cells was carried out using TRIzol reagent in accordance with the instructions provided by the manufacturer. The complementary DNA (cDNA) was generated from 1  $\mu\text{g}$  of RNA utilizing the PrimeScript™ RT reagent kit (#RR047A; Takara, Beijing, China). The study conducted an amplification reaction using TB Green® Premix Ex Taq™ (#RR420A; Takara) and gene specific primers (Table S1) on an Applied Biosystems ViiA 7 system (Applied Biosystems, Foster, CA, USA) following the manufacturer's protocol. The amplification reaction

consisted of one cycle at 95 °C for 30 s, followed by forty cycles of 95 °C for 5 s and 60 °C for 30 s. The internal control utilized in the study was  $\beta$ -actin.

### 2.11. Nrf2-ARE binding assay

The assay for Nrf2-ARE binding was performed using the ARE reporter kit (#60514; BioScience, San Diego, CA, USA) following the manufacturer's protocol. Briefly, HEK293T cells (5,000 cells/well) were seeded into a white clear-bottom 96-well plate and allowed to adhere overnight. The cells were transfected with 1  $\mu\text{L}$  of ARE reporter (60 ng DNA/ $\mu\text{L}$ , ARE luciferase reporter vector and constitutively expressing *Renilla* luciferase vector) or negative control reporter (non-inducible luciferase vector and constitutively expressing *Renilla* luciferase vector) for 24 h. Subsequently, the cells were treated with indicated DNQ or equivalent concentration of DMSO (control) for another 24 h at 37 °C. The dual luciferase assay for Nrf2-ARE binding was performed using a dual-luciferase reporter assay system (#E1910; Promega).

### 2.12. Cellular thermal shift assay

The cultured AML12 cells were lysed on ice for 10 min through the utilization of RIPA lysis buffer which contained PMSF and protease inhibitor cocktail. After centrifugation (12,000 g) at 4 °C for 10 min, cell lysates were incubated with or without 1  $\mu\text{M}$  DNQ under shaking at 4 °C overnight. The protein concentration was ascertained through employment of a BCA protein assay kit and subsequently standardized to 2  $\mu\text{g}/\mu\text{L}$  by means of RIPA lysis buffer. Fifty microliters of cellular lysates were aliquoted into fresh tubes and subjected to thermal treatment for 2.5 min per tube at varying temperatures ranging from 48 to 78 °C, utilizing a thermal mixer C (Eppendorf, Framingham, MA, USA). Following centrifugation at 12,000 g for 10 min, 40  $\mu\text{L}$  of the resulting supernatants were subjected to incubation with 10  $\mu\text{L}$  of 5  $\times$  SDS-PAGE loading buffer at 95 °C for 10 min prior to conducting a Western blot assay.

### 2.13. Biotin-dPEG<sup>®</sup>3-MAL (BPM)-precipitation assay

The BPM-precipitation assay was conducted on RAW264.7 and AML12 cells, as per the methodology reported earlier [26]. Briefly, cellular lysis was performed utilizing RIPA lysis buffer supplemented with PMSF and a protease inhibitor cocktail. The protein concentration of the resulting cell lysates was standardized to 2  $\mu\text{g}/\mu\text{L}$  using RIPA lysis buffer. The cell lysates were subjected to a 30 min incubation at room temperature with DNQ (ranging from 0.1 to 10  $\mu\text{M}$  in Tris-HCl, pH 7.6), followed by a subsequent 30 min incubation at 37 °C with a 10-fold concentration of BPM. The mixture was subjected to reaction with biotin at a temperature of 4 °C for the duration of one night, with the inclusion of avidin agaroses. Following centrifugation, the resultant supernatants were transferred into fresh tubes, while the precipitated agarose beads were subjected to two washes with 1 mL of RIPA buffer. The Keap1 protein levels were assessed through Western blot in both the supernatants and precipitations.

### 2.14. Plasmid amplification, extraction and transfection

The plasmids pCDNA3-Myc3-Nrf2, pCDNA-Flag-Keap1, and mRFP-Ub were obtained from Addgene (Watertown, MA, USA). The pCDNA-Flag-Keap1-C288A mutant, pCDNA-Flag-Keap1-C257A mutant, pCDNA-Flag-Keap1-C489A mutant, and pCDNA-Flag-Keap1-C297A mutant were procured from YouBio Biotechnology (Changsha, China). The plasmids were amplified in *Escherichia coli*

that were cultured in lysogeny broth supplemented with the appropriate antibiotic resistance. Subsequently, the bacterial liquid was utilized to extract the plasmid using a kit (#12163; QIAGEN, Shanghai, China) in accordance with the manufacturer's instruction. The concentration of DNA in plasmids was assessed using a Nanovue Spectrophotometer (Biochrom, MA, USA). The HEK293T cells were cultured in a 24-well or 6-well plate and allowed to reach a 70% cell confluence. The transfection process involved the use of lipofectamine™ 3,000 transfection reagent to introduce single or multiple plasmids per well into the cells, following the manufacturer's protocol.

The Nrf2 shRNA (m) lentiviral particles (# sc-37049-V), heme oxygenase 1 shRNA (m) lentiviral particles (#sc-35555-V), control shRNA lentiviral particles (#sc-108080) and polybrene (#sc-134220) were procured from Santa Cruz Biotechnology (Dallas, TX, USA). BV2 cells were cultured in a 24-well plate until reaching a 60% cell confluence. Subsequently, the cells were treated with polybrene (5 µg/mL) for a duration of 30 min, followed by exposure to shRNA (m) lentiviral particles for a period of 24 h. The efficacy of the knock-down was validated through qPCR and Western blot analysis prior to subsequent experiments.

### 2.15. RNA sequencing

The RAW264.7 cells were cultured in a 60 mm cell culture dish. Upon reaching 90% confluence, the cells were subjected to incubation with DNQ (1 µM) for a duration of 6 h. Subsequently, the cells underwent two rounds of cold PBS washing and were subsequently lysed with 1 mL of Trizol reagent. The cellular lysates underwent high-throughput sequencing to capture all transcripts. The data were analyzed through the free online platform of Majorbio Cloud Platform ([www.majorbio.com](http://www.majorbio.com)).

### 2.16. Co-immunoprecipitation (Co-IP) assay

The Co-IP technique was employed to identify the physical association between Nrf2 and Keap1. HEK293T cells were transfected with Myc3-Nrf2 plasmid together with plasmids of Flag-Keap1 or Flag-Keap1-C489A mutant using lipofectamine 3,000 transfection reagent following the manufacturer's procedure. Prior to conducting additional experiments, the Western blot assay was utilized to verify the transfection efficiency. Cells that underwent successful transfection were placed into a culture dish with a diameter of 60 mm. When the cells reached 80% confluence, they were incubated for an additional 12 h in the presence or absence of 1 µM DNQ. The cells were lysed with non-reduced RIPA lysis containing PMSF and protease inhibitor cocktail on ice for 10 min, and then centrifuged at 12,000 g for 10 min at 4 °C. The protein concentration was assessed by means of the BCA protein assay kit and subsequently standardized to 1 µg/µL utilizing RIPA lysis buffer. The total protein expression in the cells was measured with anti-Nrf2, anti-Keap1, anti-Myc, and anti-Flag antibodies, and Keap1-Nrf2 complex was detected in the immunoprecipitants immunoprecipitated by anti-Myc magnetic beads or protein A/G PLUS-agarose.

### 2.17. DNQ-NAC chemical reaction identification

Initially, an examination was conducted on the interaction between NAC and DNQ across various cell lines (A549, AML12, RAW264.7) cultivated in distinct culture media (RPMI-1640, DMEM/F12, DMEM). The cells were cultured in a 6 well plate overnight and subsequently treated with 177.5 ng/mL DNQ with or without 500 µM NAC for 6 h. Subsequently, the ultra-performance liquid chromatography (UPLC) analysis ([Supplementary Method 1](#))

was utilized to evaluate the alterations in DNQ concentration in the supernatants. Thereafter, an examination was conducted on the reaction routes involving NAC and DNQ. DNQ and NAC were solubilized in methanol and subjected to incubation at 37 °C for 12 h. Subsequently, the reaction products underwent UPLC analysis, and the purified reaction products were characterized using UPLC-time-of-flight mass spectrometry (UPLC-TOF-MS) and nuclear magnetic resonance (NMR) techniques.

NMR spectra were recorded on a Bruker Avance-600 (Bruker, Switzerland; 600 MHz for <sup>1</sup>H NMR, 150 MHz for <sup>13</sup>C NMR) NMR spectrometer, with the chemical shift values presented as δ values having tetramethylsilane (TMS) as an internal standard. Spectra generated from a solution of Pyridine-*d*<sub>5</sub> and Methanol-*d*<sub>4</sub> were referenced to residual pyridine (δH: 8.52, 7.22, 7.65 ppm; δC: 150.3, 124.1, 135.9) and to residual methanol (δH: 3.31 ppm; δC: 49.0), respectively. Compound **1** (DNQ, C<sub>15</sub>H<sub>12</sub>N<sub>2</sub>O<sub>4</sub>): high resolution mass spectrometry (HRMS): 285.0979 [M+H]<sup>+</sup>. <sup>1</sup>H NMR (600 MHz, Pyridine-*d*<sub>5</sub>): δ 6.84 (s, 1H), 6.79 (s, 1H), 4.03 (s, 3H), 2.60 (s, 3H), 2.56 (s, 3H). <sup>13</sup>C NMR (150 MHz, Pyridine-*d*<sub>5</sub>): δ 182.88, 177.34, 162.86, 162.02, 151.04, 149.80, 141.99, 127.77, 127.35, 118.72, 115.32, 34.48, 23.58, 22.68; Compound **2** (DNQ-C7-NAC, C<sub>20</sub>H<sub>19</sub>N<sub>3</sub>O<sub>7</sub>S): HRMS: 446.1039 [M+H]<sup>+</sup>. <sup>1</sup>H NMR (600 MHz, Pyridine-*d*<sub>5</sub>): δ 6.80 (s, 1H), 5.34 (td, *J* = 7.7, 5.0 Hz, 1H), 4.31 (dd, *J* = 13.9, 5.0 Hz, 1H), 4.07 (dd, *J* = 13.9, 7.7 Hz, 1H), 4.03 (s, 3H), 3.05 (s, 3H), 2.53 (s, 3H), 2.16 (s, 3H); Compound **4** (DNQ-2NAC, C<sub>25</sub>H<sub>26</sub>N<sub>4</sub>O<sub>10</sub>S<sub>2</sub>): HRMS: 607.1184 [M+H]<sup>+</sup>. <sup>1</sup>H NMR (600 MHz, Pyridine-*d*<sub>5</sub>): δ 5.38 (td, *J* = 7.7, 5.0 Hz, 1H), 5.34 (td, *J* = 7.7, 5.0 Hz, 1H), 4.38 (dd, *J* = 13.9, 4.8 Hz, 1H), 4.33 (dd, *J* = 13.9, 4.8 Hz, 1H), 4.15 (dd, *J* = 13.9, 7.6 Hz, 1H), 4.10 (dd, *J* = 13.9, 7.6 Hz, 1H), 4.03 (s, 3H), 2.99 (s, 6H), 2.18 (s, 6H). <sup>13</sup>C NMR (150 MHz, Methanol-*d*<sub>4</sub>): δ 183.74, 176.58, 173.80, 173.78, 173.25, 173.21, 162.15, 161.89, 154.92, 153.31, 140.09, 139.25, 134.34, 134.15, 121.55, 117.14, 54.30, 54.26, 49.71, 35.71, 35.23, 35.14, 22.59, 21.80, 20.96; Compound **3** (DNQ-C3-NAC, C<sub>20</sub>H<sub>19</sub>N<sub>3</sub>O<sub>7</sub>S): HRMS: 446.1039 [M+H]<sup>+</sup>. We did not obtain the NMR data of compound **3**. The chemical structure of this compound was deduced according to the HRMS of compound **3**, combined with the <sup>1</sup>H NMR and <sup>13</sup>C NMR of compound **2** and compound **4**.

### 2.18. DNQ-Linker (DNQ-L) probe synthesis and pull-down assay

The process of synthesizing, purifying, and identifying the DNQ-L probe was carried out using [Supplementary Method 2](#).

The pull-down assay is a commonly used experimental technique in biochemistry and molecular biology to investigate protein-protein interactions. HEK293T cells, either normal or overexpressed Keap1, were subjected to lysis using RIPA lysis buffer supplemented with PMSF and a protease inhibitor cocktail. Following centrifugation, the resulting supernatants were subjected to incubation with DNQ-L (2 µM) at 4 °C for a duration of 12 h. Subsequently, biotin-PEG3-azide was introduced into the mixture to facilitate click chemistry reaction, as per the guidelines outlined in [Supplementary Method 3](#). Thereafter, avidin agarose beads were introduced into the cellular lysates to isolate the DNQ-protein complex that had been bound to biotin. Following centrifugation at 12,000 g for 10 min, the supernatants and precipitates were subjected to boiling with 5 × SDS-PAGE loading buffer at 95 °C for 10 min prior to Western blot analysis.

### 2.19. Liquid chromatography-tandem mass spectrometry (LC-MS/MS) for the DNQ-Keap1 binding sites analysis

This section contains four steps: Protein binds to small molecule; Protein digestion; Nano LC-MS/MS analysis; Data analysis. The procedures are illustrated in [Supplementary Method 4](#).

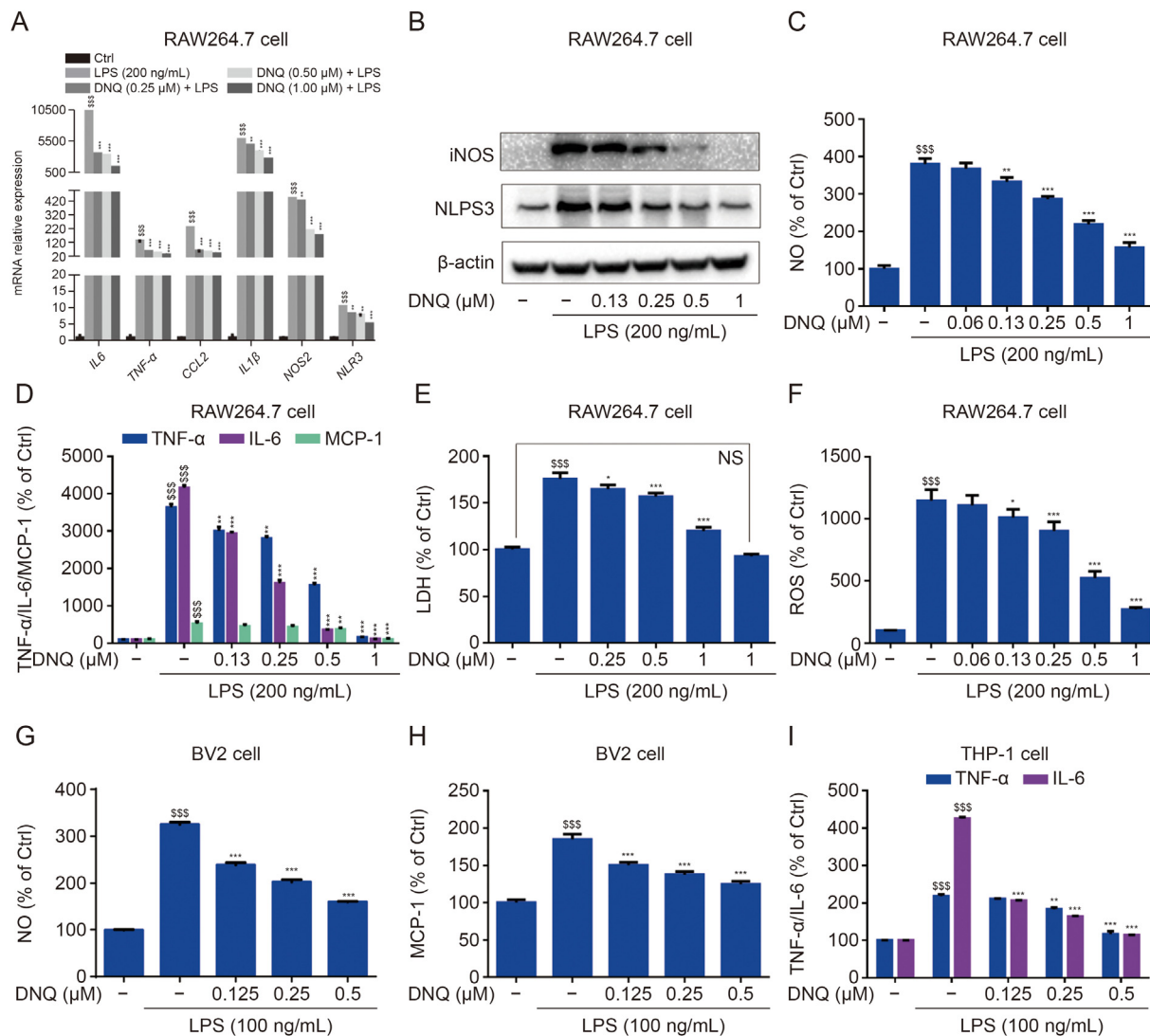


**Fig. 1.** Deoxyxyboquinone (DNQ) showed potent anti-inflammatory effects *in vitro*. (A) mRNA levels of inflammatory genes (*Il6*, *Tnfα*, *Ccl2*, *Il1β*, *Nos2*, *Nlrp3*;  $n = 6$ ), (B) pro-inflammatory proteins (iNOS, NLRP3), (C) nitric oxide (NO;  $n = 6$ ), (D) pro-inflammatory cytokines (tumor necrosis factor alpha (TNF- $\alpha$ ), interleukin-6 (IL-6), monocyte chemoattractant protein-1 (MCP-1);  $n = 5$ ), (E) lactate dehydrogenase (LDH;  $n = 5$ ), and (F) the intracellular reactive oxygen species (ROS;  $n = 5$ ) were detected to be reduced by DNQ in lipopolysaccharides (LPS)-induced RAW264.7 cells for 12 h. DNQ limited the (G) NO ( $n = 6$ ) and (H) MCP-1 ( $n = 5$ ) in LPS-induced BV2 microglial cells for 12 h. DNQ limited the (I) pro-inflammatory cytokines (TNF- $\alpha$ , IL-6;  $n = 5$ ) in LPS-induced human THP-1 macrophages for 12 h.  $^{SSS}P < 0.001$  vs. the Ctrl group.  $^*P < 0.05$ ,  $^{**}P < 0.01$  and  $^{***}P < 0.001$  vs. the LPS group. Ctrl: control.

## 2.20. Animal experiment

The male C57/BL6 mice used in this study were 7–8 weeks old and were obtained from the Animal Facility at the Faculty of Health Sciences, University of Macau. The mice were kept in a standard animal laboratory environment [27]. The experimental protocols with reference numbers UMARE-025-2021 and UMARE-AMEND-173 followed the National Institutes of Health guidelines for the Care and Use of Laboratory Animals. These protocols were also approved by the Animal Research Ethics Committee of the University of Macau.

### 2.20.1. Acute toxicity observation

Twenty-four mice were randomly divided into four groups: Control (Ctrl), DNQ 0.5, DNQ 1, and DNQ 2 mg/kg. The mice were administered intravenously daily at day 1, day 3, and day 5. The body weight of each mouse was monitored daily for a week. On the seventh day, the mice were euthanized by inhaling CO<sub>2</sub>. Blood

samples were collected to perform a blood chemistry assay, which included measuring the levels of alkaline phosphatase (ALP), aspartate transaminase (AST), and alanine transaminase (ALT). Additionally, the liver, kidney, and lung were isolated for pathological analysis using hematoxylin-eosin staining.

### 2.20.2. Peritoneal macrophages assay

Ten mice were separated into two groups randomly. Then, the mice were intraperitoneally administrated with 1 mg/kg DNQ and vehicle (25% PEG400 in saline). The peritoneal macrophages were collected at 6 h for qPCR and Western blot assays.

### 2.20.3. Endotoxin-induced acute inflammation model

To measure cytokines and spleen index, a group of six mice were treated intravenously with DNQ (at doses of 0.25, 0.5, and 1 mg/kg), dimethyl fumarate (at a dose of 10 mg/kg), and a vehicle (consisting of 25% PEG400 in saline) for a period of 2 h. After this, the mice were stimulated with LPS (at a dose of 2 mg/kg, administered

intraperitoneally) for a period of 4 h. After conducting the experiments, we collected the serum to determine the cytokines and isolated the spleen to calculate the spleen index. Furthermore, the body temperature of six mice subjected to the same treatment was measured using an infrared thermometer (Pluto, Guangzhou, China) at 0, 2, 6, 12, and 24 h after DNQ administration.

### 2.21. Statistical analysis

All data are expressed as the mean  $\pm$  standard deviation (SD). Results are representative examples of at least three individual experiments. The Student's *t*-test was used to compare two groups. One-way analysis of variance (ANOVA) followed by Dunnett's test was used to compare three and more groups ( $P < 0.05$  was considered statistically significant difference, NS means not significant). GraphPad Prism was used for analysis.

## 3. Results

### 3.1. DNQ exhibited potent anti-inflammatory effects in vitro and in vivo

The toxicity of DNQ was evaluated through *in vitro* (as shown in Fig. S1B) and *in vivo* (as demonstrated in Fig. S2) experiments. At the non-toxic concentrations ranging from 0.06 to 1  $\mu$ M, DNQ was observed to dose-dependently inhibit the inflammatory responses in LPS-stimulated RAW264.7 macrophages. The mRNA levels of inflammatory genes (*Nos2*, *Nlrp3*, *Il1 $\beta$* , *Il6*, *Tnf $\alpha$*  and *Ccl2*; Fig. 1A), expression of proinflammatory proteins (iNOS and NLRP3; Fig. 1B), extracellular release of NO (Fig. 1C), secretion of proinflammatory cytokines (interleukin (IL)-6, tumor necrosis factor alpha (TNF- $\alpha$ ) and monocyte chemoattractant protein-1 (MCP-1); Fig. 1D) and LDH

(Fig. 1E), as well as the intracellular production of reactive oxygen species (Fig. 1F) were all detected to be significantly decreased by DNQ under a concentration at nanomolar level. The similar effects were also observed in LPS-stimulated BV2 microglial cells (Figs. 1G and H) and differentiated-human THP-1 macrophages (Fig. 1I). Furthermore, the *in vivo* experiments demonstrated that DNQ at doses of 0.25, 0.5, and 1.0 mg/kg effectively mitigated the decrease in 24 h body temperature (Fig. 2A), decreased spleen enlargement (Fig. 2B), and lowered serum cytokine levels (IL-6, IL-8, MCP-1, and interferon gamma (IFN- $\gamma$ ); Figs. 2C–F) in mice with acute inflammation induced by LPS. DNQ (1.0 mg/kg) exhibited a comparable inflammation-suppressing capability to the positive drug dimethyl fumarate (10 mg/kg) (Fig. 2).

### 3.2. Two $\alpha$ , $\beta$ -unsaturated amides moieties were the pharmacophore of DNQ on HO-1 upregulation and inflammation inhibition

To investigate the potential anti-inflammatory mechanisms, transcriptome sequencing (RNA-seq) of DNQ-treated macrophages was utilized to analyze the potential targets. The results indicated that *Hmox1* was the predominantly upregulated anti-inflammatory gene in DNQ-incubated RAW264.7 macrophages (Table S2), which was similar to the previous report that DNQ upregulated *Hmox1* gene expression (the Top 1 upregulated gene) in U-937 human myeloid leukaemia cells [13]. Furthermore, the HO-1 protein (encoded by the *Hmox1* gene) expression was also detected to be dose-dependently upregulated by DNQ in RAW264.7 macrophages (Fig. 3A) and U-937 cells (Fig. 3B). HO-1 is a stress-response protein and plays a prominent role in cellular responses to oxidative stress and inflammation [28–30]. Upregulation of HO-1 expression has been demonstrated to

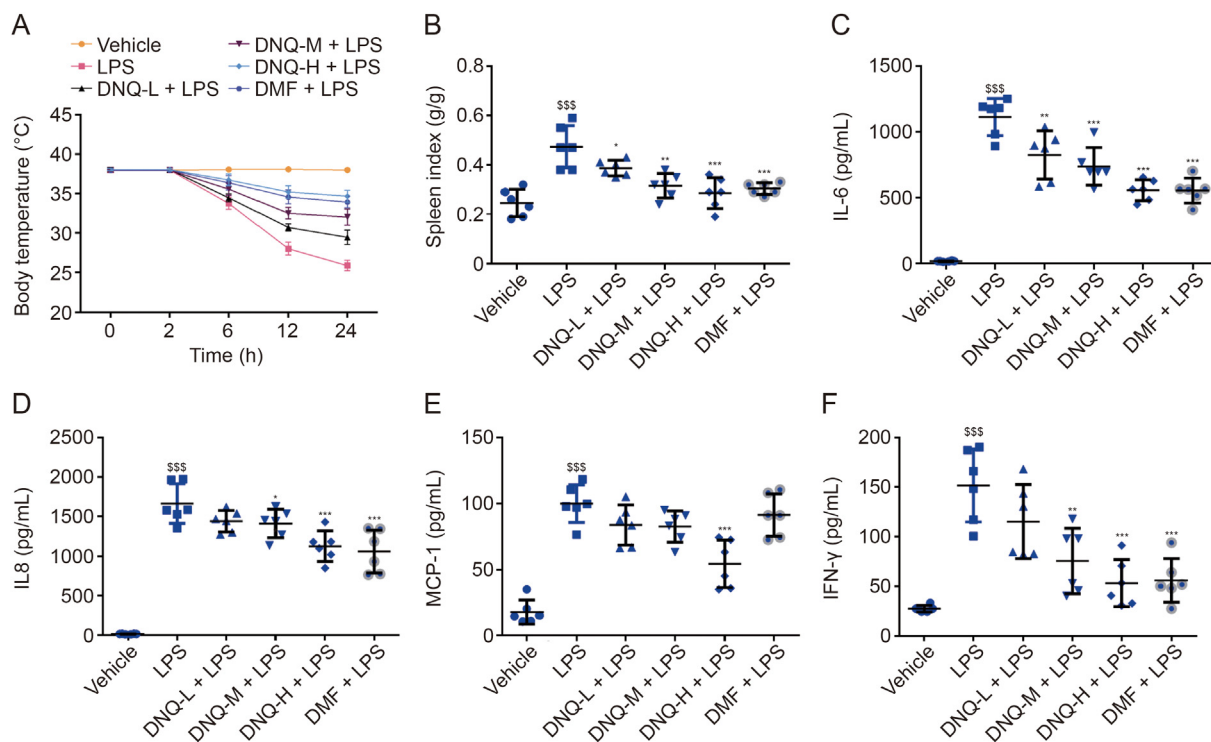


**Fig. 2.** Deoxyxyboquinone (DNQ) counteracted lipopolysaccharides (LPS)-induced pro-inflammatory response in mice. Mice were intravenously pre-treated with DNQ (DNQ-L, 0.25 mg/kg; DNQ-M, 0.5 mg/kg; DNQ-H, 1 mg/kg), positive drug dimethyl fumarate (DMF; 10 mg/kg) and vehicle (25% PEG400 in saline) for 2 h, then administered intraperitoneally with LPS (2 mg/kg) for indicated times. (A) The body temperatures were monitored at 0, 2, 6, 12 and 24 h after DNQ treatment ( $n = 6$ ). (B) Spleen index and serum inflammation-related cytokines including (C) interleukin-6 (IL-6), (D) interleukin-8 (IL-8), (E) monocyte chemoattractant protein-1 (MCP-1), and (F) interferon gamma (IFN- $\gamma$ ) were determined in the 6th h after the same drugs administration in another independent experiment ( $n = 6$ ).  $^{s}P < 0.001$  vs. the Ctrl group.  $^{*}P < 0.05$ ,  $^{**}P < 0.01$ ,  $^{***}P < 0.001$  vs. the LPS group. Ctrl: control.

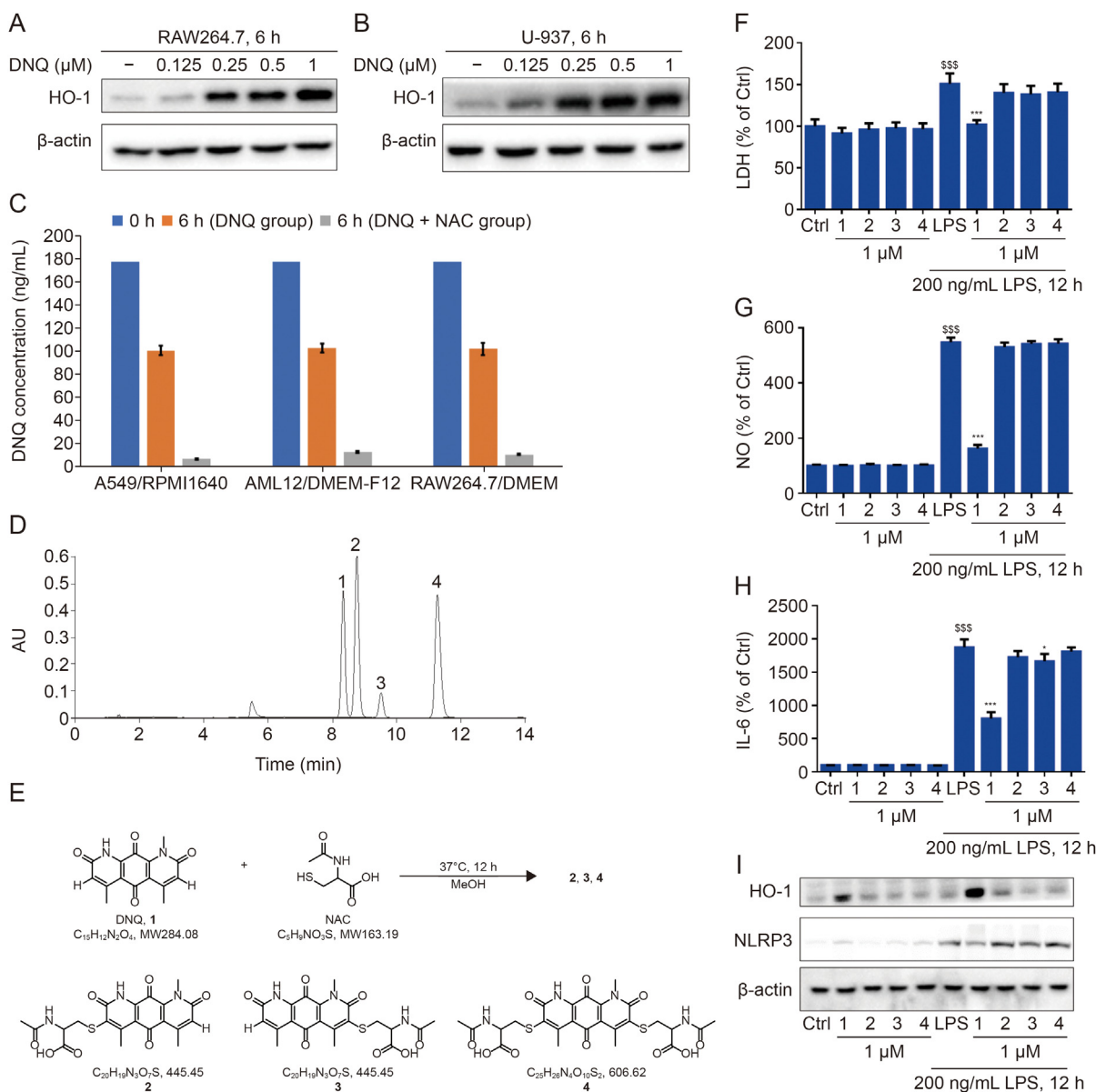


**Fig. 3.** Two  $\alpha$ ,  $\beta$ -unsaturated amides moieties were the pharmacophore of deoxyxyloquinone (DNQ) for heme oxygenase 1 (HO-1) upregulation and inflammation inhibition. (A) DNQ dose-dependently induced HO-1 expression in RAW264.7 cells, detected by Western blot. (B) DNQ dose-dependently induced HO-1 expression in U-937 cells, detected by Western blot. (C) Concentration of DNQ was decreased in the presence of *N*-acetylcysteine (NAC) regardless of the cell types and culture media. The cells (A549, AML12 and RAW264.7) were seeded in a 6-well culture plate with different media (RPMI-1,640, DMEM-F12 and Dulbecco's modified Eagle's medium (DMEM)) overnight, then 177.5 ng/mL of DNQ was added into each well in the presence or absence of 500  $\mu$ M NAC for 6 h, and supernatants were collected to detect the left DNQ concentration with ultra-performance liquid chromatography (UPLC) method ( $n = 5$ ). (D) Four peaks were detected by UPLC analysis when DNQ was dissolved into NAC at 37 °C for 12 h. (E) The chemical structures corresponding to the four UPLC peaks were identified to be DNQ (compound 1) and compounds 2–4. (F) All compounds (1–4) did not lead to the release of lactate dehydrogenase (LDH) while compound 1 reduced the lipopolysaccharides (LPS)-induced LDH in RAW264.7 cells ( $n = 6$ ). (G) Compound 1 but not the compounds 2–4 inhibited the production of nitric oxide (NO) in LPS-induced RAW264.7 cells ( $n = 6$ ). (H) Compound 1 but not the compounds 2–4 inhibited the secretion of interleukin-6 (IL-6) in LPS-induced RAW264.7 cells ( $n = 6$ ). (I) Compound 1 inhibited NLRP3 and upregulated HO-1 in LPS-stimulated RAW264.7 cells, but the compounds 2–4 failed to inhibit NLRP3 and upregulate HO-1.  $^{SSS}P < 0.001$  vs. the Ctrl group.  $^*P < 0.05$  and  $^{***}P < 0.001$  vs. the LPS group. Ctrl: control.

attenuate the oxidative stress- and inflammation-induced injuries [25].

Previously, DNQ was reported to lose its capacity of up-regulating HO-1 in the presence of NAC [13], we observed the similar results in RAW264.7 macrophages (data not shown). Further investigation indicated that the concentration of DNQ was significantly decreased in the presence of NAC (Fig. 3C), and this effect was observed regardless of the types of culture media or cells used. Thus, our hypothesis was that a chemical reaction occurred between DNQ and NAC. As illustrated in Fig. 3D, four peaks were detected by UPLC analysis in the

reacted mixture when dissolved the DNQ and NAC together. Subsequently, the chemical structures corresponding to the four peaks were identified in Fig. 3E by NMR spectroscopy (Figs. S3–S5). NAC was demonstrated to react partially or completely with the two  $\alpha$ ,  $\beta$ -unsaturated amides moieties in DNQ (compound 1), resulting in the products of compounds 2, 3 and 4. The reaction mechanism was involved in a conjugate addition process followed by the rearrangement of electrons, ultimately removed two hydrogens [31].

Next, we assessed the biological activities of the reaction products in terms of their ability to upregulate HO-1 and inhibit

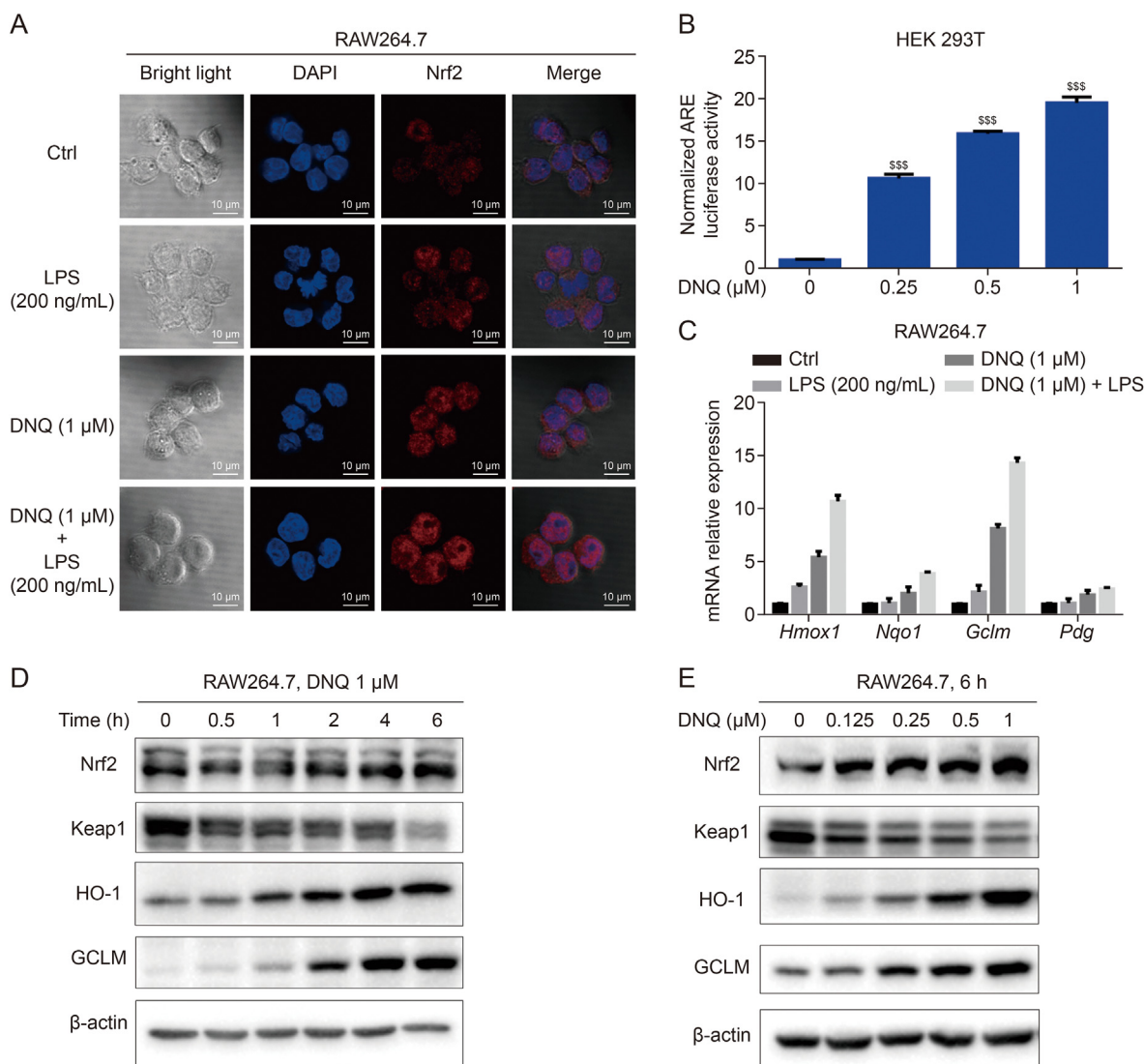


**Fig. 4.** Deoxyxyboquinone (DNQ) activated the Kelch-like ECH-associated protein 1 (Keap1)-nuclear factor erythroid 2-related factor 2 (Nrf2)-antioxidant response elements (ARE) signal pathway in the presence or absence of lipopolysaccharides (LPS)-treated RAW264.7 cells. (A) DNQ increased the stabilization and nucleus translocation of Nrf2. RAW264.7 cells were treated with DNQ with or without of LPS for 6 h, then the cells were subjected to immunofluorescence staining (blue, DAPI; red, Nrf2). (B) DNQ induced the high expression of ARE reporter in HEK293T cells. HEK293T cells were transfected with ARE reporter, then incubated with DNQ for 24 h, following by dual luciferase assay with a dual-luciferase reporter assay system ( $n = 3$ ). (C) DNQ induced genes expression in Nrf2 downstream. RAW264.7 cells were treated with DNQ for 6 h in the presence or absence of LPS, then the mRNA expression of genes (*Hmox1*, *Nqo1*, *Gclm*, and *Pdg*) in cells were detected by quantitative polymerase chain reaction (qPCR) ( $n = 5$ ). (D,E) DNQ induced the decrease of Keap1 and increase of Nrf2, heme oxygenase 1 (HO-1) and GCLM in RAW264.7 cells in a time- (D) and dose-dependent (E) manner. <sup>s</sup> $P < 0.05$ , <sup>ss</sup> $P < 0.01$  and <sup>sss</sup> $P < 0.001$  vs. Ctrl group. Ctrl: control; DAPI: 4',6'-diamidino-2-phenylindole.

inflammation. The comparative investigations showed that DNQ (compounds **1**) and compounds **2–4** at the concentration of 1 μM were noncytotoxic to RAW264.7 cells in the presence or absence of LPS (Fig. 3F). However, compounds **2–4** almost lost the ability to inhibit inflammation (Figs. 3F–I) and upregulate HO-1 (Fig. 3I) in comparison with DNQ (compounds **1**) group in LPS-induced RAW2647 macrophages. The results confirmed that DNQ contained the pharmacophore of  $\alpha$ ,  $\beta$ -unsaturated amides moieties, and this pharmacodynamic structure could be inactivated by covalently binding with the sulfhydryl group in NAC. As a result, the anti-inflammatory activities of DNQ were limited.

### 3.3. DNQ exerted anti-inflammatory effects through activation of Keap1/Nrf2/ARE signal pathway by targeting Keap1

The Keap1/Nrf2/ARE signaling pathway is widely recognized as the “power switch” for oxidative stress and is crucial in regulating

oxidative stress and inflammatory diseases [5,7]. HO-1 is a downstream protein that plays a crucial role in the Keap1/Nrf2/ARE signal pathway [32,33]. The up-regulation of HO-1 and inhibition of inflammation could be mediated by the activation of Nrf2 [25]. As illustrated in Fig. 4, DNQ increased the stabilization and nucleus expression of Nrf2 (Fig. 4A), the binding of Nrf2 to ARE (Fig. 4B), and the mRNA expressions of Nrf2 downstream genes (*Hmox1*, *Nqo1*, *Gclm* and *Pdg*; Fig. 4C) in LPS-stimulated or unstimulated RAW2647 macrophages. In addition, it was found that DNQ down-regulated Keap1 and up-regulated the expression of Nrf2, HO-1 and GCLM in the RAW264.7 macrophages in a time- and dose-dependent manner (Figs. 4D and E). These findings suggested that DNQ regulated the Keap1/Nrf2/ARE signal pathway.

The impact of DNQ on the Keap1/Nrf2 signal pathway was further confirmed in BV2 cells (Figs. 5A–C) and peritoneal macrophages derived from mice (Figs. 5D and E). Importantly, DNQ was detected to fail to up-regulate HO-1 (Fig. 6A), nor reverse the

LPS-induced production of NO (Fig. 6B) and *IL6* mRNA (Fig. 6C) when knocking down the Nrf2 with Nrf2 shRNA lentiviral particles in BV2 cells. Similarly, DNQ could partially abrogate the LPS-induced upregulation of NO (Fig. 6B) and *IL6* mRNA (Fig. 6C) when knocking down the HO-1 (Fig. 6A) or in the presence of ZnPP (HO-1 inhibitor) (Fig. 6D). The above results suggested that DNQ inhibited inflammation through activation of Keap1/Nrf2 signal pathway.

Given the critical role of Keap1 in regulating Keap1/Nrf2 signal pathway activation, we attempted to determine if DNQ triggered the activation of the Keap1/Nrf2 signaling pathway by targeting Keap1. Fig. 7A demonstrated that the isothermal titration calorimetry experiment revealed an interaction between DNQ and recombinant Keap1 protein *in vitro*. Additionally, Fig. 7B showed

that the cellular thermal shift assay indicated an interaction between DNQ and intracellular Keap1. These findings suggested that DNQ could directly target to Keap1. Our research had shown that DNQ interacted with NAC (Fig. 3E) and GSH (Fig. S6A) by targeting the sulfhydryl group. This suggested that DNQ might also target the cysteine residues of Keap1 in a similar way. This hypothesis was confirmed in Fig. S6B, which demonstrated that DNQ competitively antagonized the binding of maleimide to the sulfhydryl group in the cysteine residue of Keap1. In addition, we were able to “Fishhook” the Keap1 protein from cell lysates using a synthesized DNQ-L probe combined with click chemistry (as demonstrated in Figs. 7C–E, and Fig. S7). However, when NAC was present, the ability of DNQ-L probe to isolate Keap1 and activate the Keap1/Nrf2 signal pathway was blocked

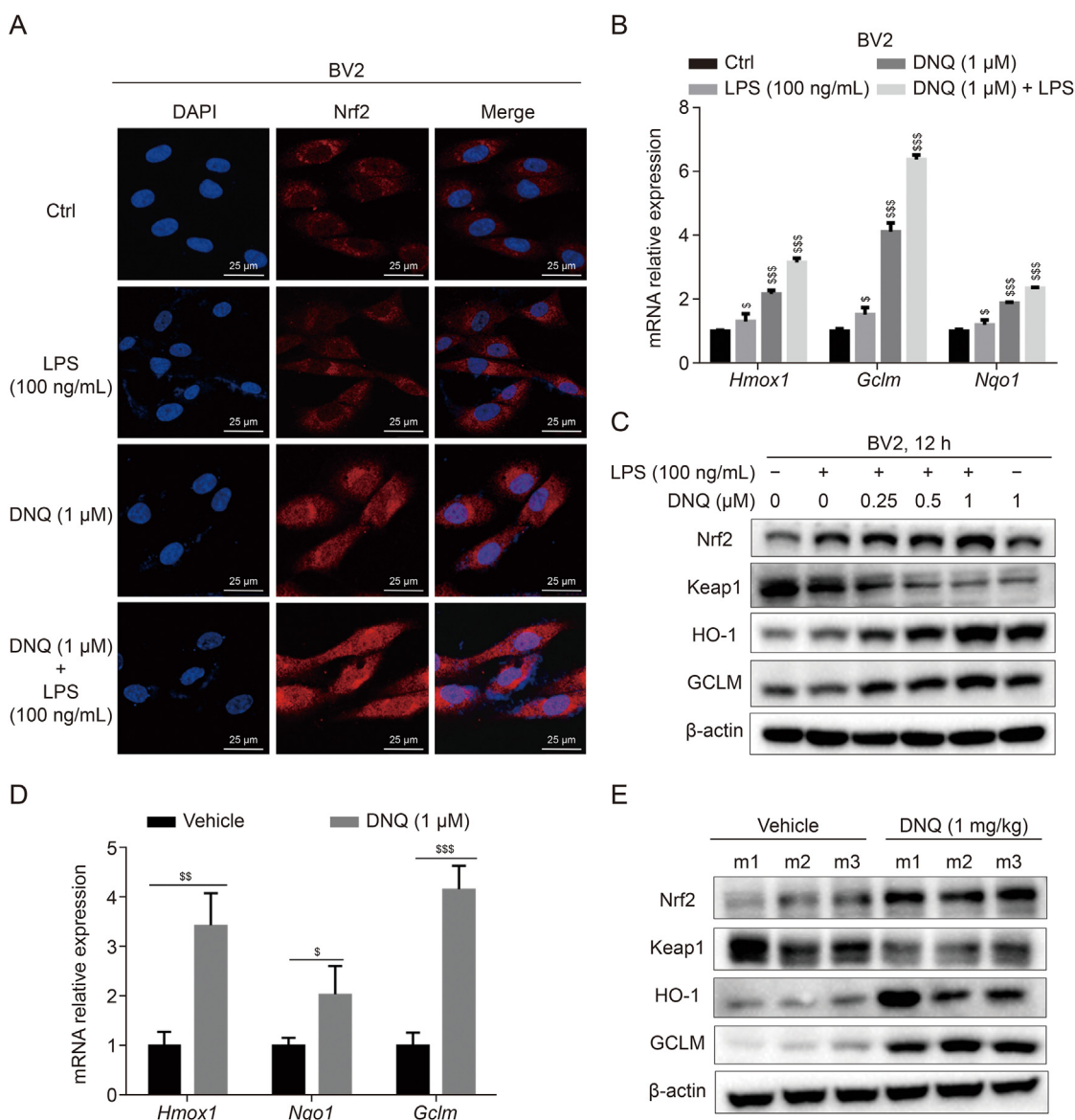


**Fig. 5.** Deoxyxyboquinone (DNQ) activated Kelch-like ECH-associated protein 1 (Keap1)-nuclear factor erythroid 2-related factor 2 (Nrf2) signal pathway in BV2 microglial cells and peritoneal macrophages. (A) DNQ increased the stabilization and nucleus translocation of Nrf2. BV2 cells were subjected to immunofluorescence staining (blue, DAPI; red, Nrf2) after treatment with DNQ in the presence or absence of lipopolysaccharides (LPS) for 6 h. (B) DNQ induced genes expression in Nrf2 downstream. BV2 cells were treated with DNQ for 6 h in the presence or absence of LPS, then the mRNA expressions of genes (*Hmxo1*, *Nqo1* and *Gclm*) in cells were detected by quantitative polymerase chain reaction (qPCR) ( $n = 5$ ). (C) DNQ induced the decrease of Keap1 and increase of Nrf2, heme oxygenase 1 (HO-1) and GCLM in BV2 cells in the presence or absence of LPS for 12 h. (D) mRNA levels of genes (*Hmxo1*, *Nqo1* and *Gclm*;  $n = 5$ ) and (E) expression of proteins (Nrf2, Keap1, HO-1 and GCLM;  $n = 3$ ) in the peritoneal macrophages derived from mice were detected. Male C57/BL6 mice ( $n = 6$ ) were intraperitoneally administered with vehicle (25% PEG40) or DNQ (1 mg/kg DNQ in 25% PEG40) for 6 h, then the peritoneal macrophages were collected for qPCR and Western blot assays.  $^{\$}P < 0.05$ ,  $^{SS}P < 0.01$  and  $^{SSS}P < 0.001$  vs. Ctrl group. Ctrl: control; DAPI: 4',6-diamidino-2-phenylindole.

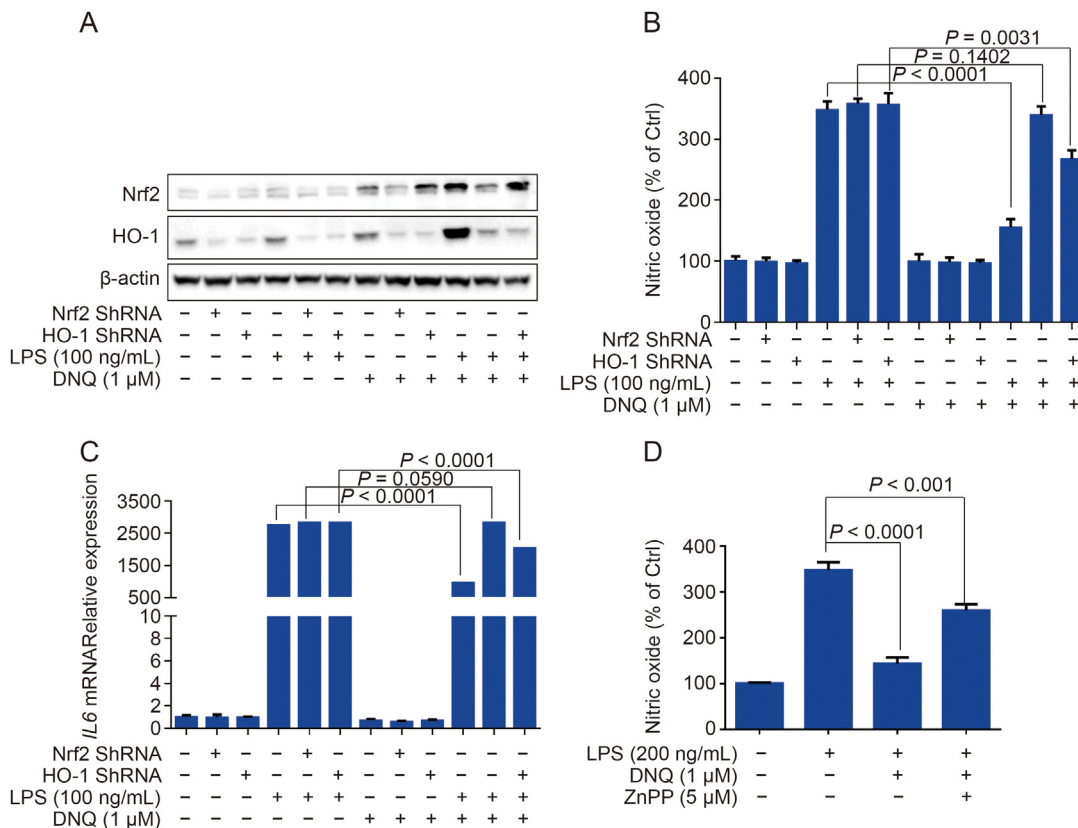


**Fig. 6.** Deoxyxyboquinone (DNQ) upregulated heme oxygenase 1 (HO-1) and inhibited inflammation in a nuclear factor erythroid 2-related factor 2 (Nrf2) dependent manner. (A) BV2 cells were seeded in 24-well plates and cultured to a 50% cell confluence, then cells were transfected with Nrf2 or HO-1 shRNA lentiviral particles for 24 h and sub-cultured in a 6-well plate. Subsequently, the cells were treated with DNQ in the presence or absence of lipopolysaccharides (LPS) for 12 h. (B) The supernatants were collected for nitric oxide (NO) release assay ( $n = 5$ ), and the cells were subjected to (A) protein (Nrf2, HO-1) and (C) *IL6* mRNA ( $n = 5$ ) assays. (D) DNQ partially inhibited the NO production in the presence of ZnPP (HO-1 inhibitor) in LPS-stimulated RAW264.7 cells for 12 h ( $n = 5$ ).

(Figs. 7D and F). The results showed that NAC competitively inhibited the binding of DNQ to the cysteine residue on Keap1. As a result, the activation of the Keap1/Nrf2 signal pathway by DNQ was blocked.

### 3.4. Cysteine 489 on Keap1 was the indispensable site for DNQ to activate the Keap1/Nrf2 signal pathway

To determine which cysteine residues were involved in the interaction between DNQ and Keap1, we conducted a liquid chromatography-mass spectrometry (LC-MS) analysis to quantify the number of DNQ molecules that could bind to the Keap1 protein. Fig. S8A demonstrated that Keap1's molecular weight ( $m/z$  98289.1) differed from that of DNQ-bound Keap1 ( $m/z$  99431.2), suggesting that Keap1 bound to 4 DNQ molecules. We performed LC-MS/MS analysis after protease cleavage to identify the cysteine residues that were specifically modified by DNQ *in vitro*. In Fig. 8A, the MS analysis of the chymotryptic peptide indicated a mass increase of 282.064, indicating that DNQ modified cysteine 489 (Cys489) through a similar addition reaction as DNQ to NAC (Fig. 3E), which removed two hydrogens. The MS results (Table S3 and Fig. S8B) revealed that covalent modifications of DNQ to Cys257, Cys288, and Cys297 were also discovered.

Since the locations of the four DNQ-ligand cysteine residues were different in Keap1 (IVR domain: Cys257, Cys288 and Cys297, and Kelch domain: Cys489), they might have different effects upon the DNQ modification. Thus, the mono-mutated Keap1, where an

individual cysteine residue was replaced with an alanine residue, was utilized to assess the significance of site-modification of Keap1 in relation to DNQ function. Fig. 8B demonstrated that all mono-mutated Keap1 plasmids were effectively transfected and expressed in HEK293T cells. However, in Fig. 8C, it was observed that the DNQ-L was barely able to pull down the Cys257- and Cys489-mutated Keap1, indicating a loss of binding capability between DNQ and these mutated forms of Keap1. Additionally, we found that DNQ had similar effects on activating the Keap1/Nrf2 signal pathway (Fig. 8D) and inhibiting *IL6* mRNA expression (Fig. 8E) in various groups, including the vector, wild type (WT) Keap1, Keap1-Cys257 mutant, Keap1-Cys288 mutant, and Keap1-Cys297 mutant groups. However, we observed that DNQ lost its effects in the Keap1-Cys489 mutant group. Therefore, Cys489 was the indispensable site for DNQ to activate Keap1/Nrf2 signal pathway in inhibiting inflammation.

### 3.5. DNQ-mediated alkylation of Keap1-Cys489 triggered the dissociation of Keap1-Nrf2 complex and the degradation of Keap1 by driving Keap1-ubiquitination

Keap1 is a negative regulator of Nrf2 through binding with Nrf2. Modification on the cysteine residues of Keap1 could disrupt the interaction between Nrf2 and Keap1, thus releasing Nrf2 into cellular nucleus to mediate anti-oxidation and anti-inflammation [5]. In the four DNQ-modified cysteine residues, Cys257, Cys288 and Cys297 are located in the IVR domain, while the Cys489 is located in the Kelch

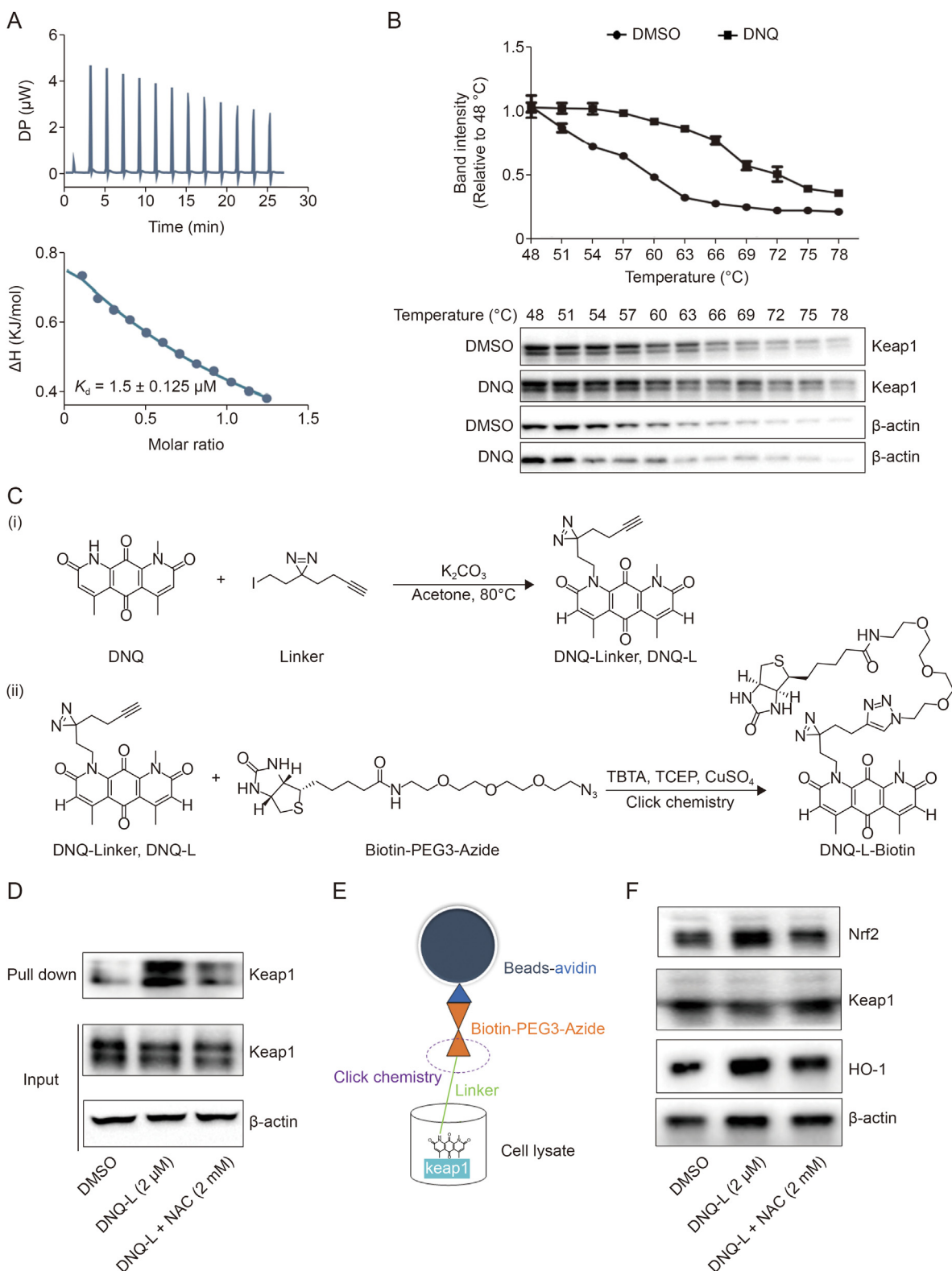


**Fig. 7.** Deoxyxyboquinone (DNQ) exerted anti-inflammatory effects through activation of nuclear factor erythroid 2-related factor 2 (Nrf2) signal pathway via directly targeting Keap1. (A) DNQ bound with human recombinant Kelch-like ECH-associated protein 1 (Keap1) protein with a binding constant ( $K_d$ ) =  $1.5 \pm 0.125 \mu\text{M}$  by isothermal titration calorimetry experiment. (B) Cellular thermal shift assay suggested the interaction between DNQ and Keap1. AML12 cells lysates were incubated with DNQ ( $1 \mu\text{M}$ ) at  $4^{\circ}\text{C}$  overnight, then  $50 \mu\text{L}$  of cellular lysates were aliquoted into fresh tubes and subjected to thermal treatment for 2.5 min at varying temperatures ( $48\text{--}78^{\circ}\text{C}$ ), utilizing Eppendorf ThermoMixer C, then the Keap1 in the supernatants was detected by Western blot ( $n = 3$ ). (C) Schemes for the synthesis of DNQ-L probe (i) and functionalization with biotin-PEG3-azide in cell lysates (ii). (D) DNQ-Linker (DNQ-L) probe was able to "fishhook" the Keap1 protein from the cell lysates. BV2 cells were lysed with radioimmunoprecipitation assay (RIPA) buffer containing phenylmethylsulfonyl fluoride (PMSF) and protease inhibitor cocktail, and the supernatants of the lysates were divided into two parts. One part was used for the input analysis, and the other part was incubated with DNQ-L probe in the presence or absence of *N*-acetylcysteine (NAC) at  $4^{\circ}\text{C}$  for 12 h. Then the biotin-PEG3-azide was added into the cell lysates to bind with the DNQ-L through a click chemistry reaction. Thereafter, the avidin agaroses were added into the cell lysates to bind with the biotin at  $4^{\circ}\text{C}$  for 12 h under

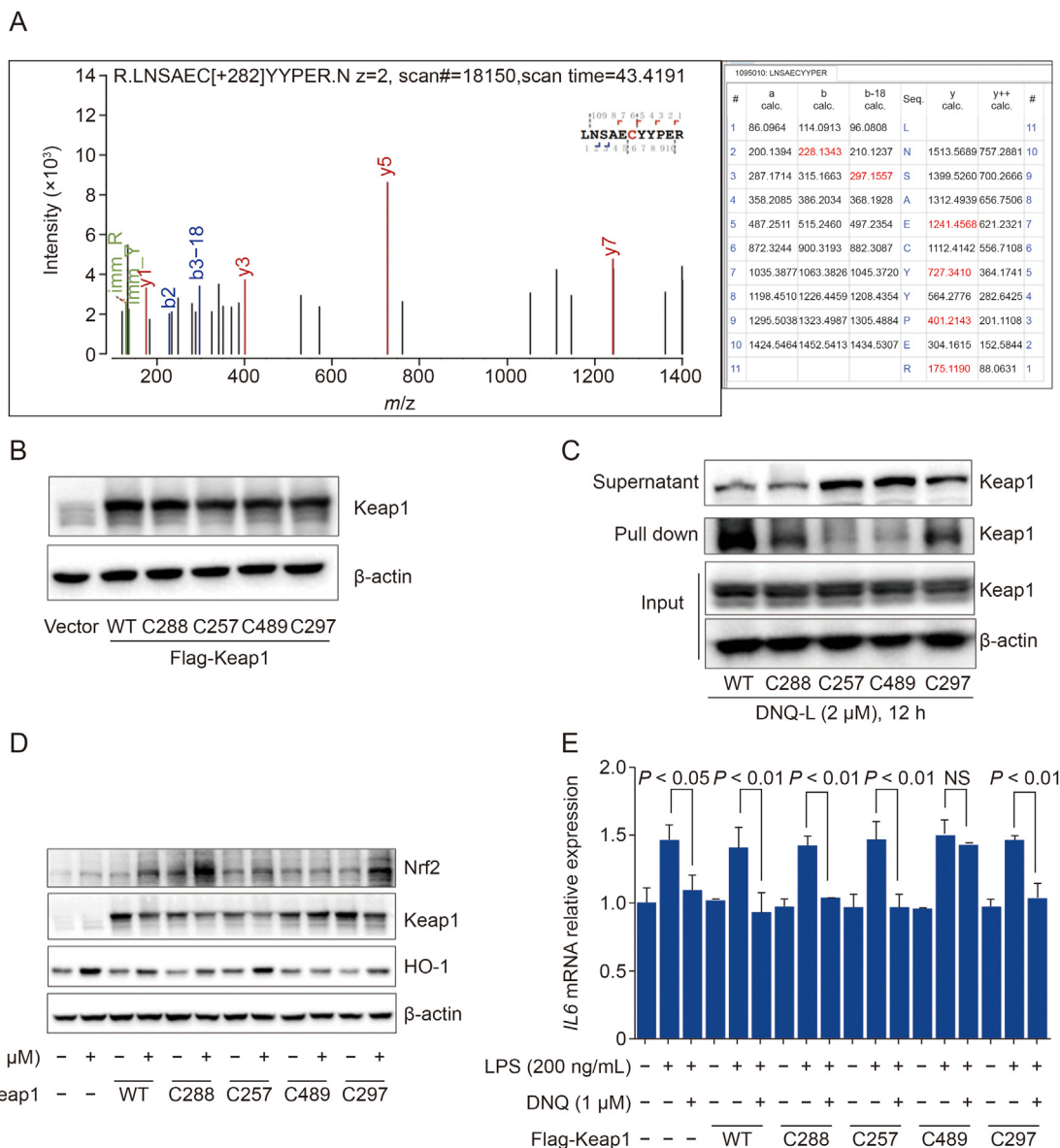


**Fig. 8.** Cys489 was the indispensable site for deoxyhydroquinone (DNQ) to activate Keap1-nuclear factor erythroid 2-related factor 2 (Nrf2) signal pathway and inhibit inflammation. (A) Tandem mass spectrometry (MS/MS) data of DNQ-modified peptide at Cys489 from Keap1. The human recombinant Keap1 was incubated with DNQ (protein-to-compound molar ratio, 1:10) at 37 °C for 12 h prior to MS analysis (left: MS/MS spectrum; right: list of the main fragments in MS/MS spectrum). (B) Successful overexpression of Flag-Keap1 proteins in HEK293T cells. HEK293T cells were transfected with vector, wild type (WT) and mutant Keap1 plasmids for 24 h at a 6-well plate, and the expression of proteins in cells were detected by Western blot. (C) Binding capacity of DNQ to different cysteines-mutant Keap1 by pull-down assay with DNQ-Linker (DNQ-L) probe. HEK293T cells, successfully transfected with WT or mutant Keap1 plasmids, were subjected to lysis utilizing radioimmunoprecipitation assay (RIPA) lysis buffer. Following centrifugation, the resulting supernatants were subjected to incubation with DNQ-L at 4 °C for 12 h. Subsequently, biotin-PEG3-azide was introduced into the mixture to facilitate click chemistry reaction. Then, avidin agarose beads were introduced into the cellular lysates to isolate the biotin-DNQ-protein complex. Following centrifugation, the supernatants and precipitates were subjected to boiling with 5 × sodium dodecyl sulphate-polyacrylamide gel electrophoresis (SDS-PAGE) loading buffer at 95 °C for 10 min prior to Western blot analysis. (D) DNQ failed to activate Keap1/Nrf2 in Cys489-mutated group. The HEK293T cells were transfected with vector, WT and mutant Keap1 plasmids for 24 h at a 6-well plate, and the cells were sub-cultured in two 6-well plates. After incubation in the presence or absence of DNQ for 6 h, the expression of proteins in cells was detected by Western blot. (E) DNQ failed to inhibit lipopolysaccharides (LPS)-induced *IL6* mRNA expression in Cys489-mutated group. The HEK293T cells were transfected with vector, WT and mutant Keap1 plasmids for 24 h at a 6-well plate. The cells were sub-cultured in three 6-well plates and then incubated with DNQ for 6 h in the presence or absence of LPS, and the *IL6* mRNA was analyzed by qPCR ( $n = 6$ ). HO-1: heme oxygenase 1.

domain (Fig. S1C). Mesecar and co-workers [34] revealed that specific modifications on Cys257, Cys288 and Cys297 (all in the IVR domain) were insufficient to disrupt the binding of Nrf2 to Keap1, while the covalent modification of Cys77 (in the BTB domain) and Cys434 (in the Kelch domain) could dissociate the Keap1-Nrf2 complex [35].

Since Cys489 is also located in the Kelch domain, DNQ might influence the interaction between Keap1 and Nrf2 by targeting the Cys489 residue.

To investigate the impact of DNQ on the interaction of Keap1 and Nrf2, HEK293T cells were transfected with Myc-Nrf2 plasmid

mixing. After removing the supernatants by centrifugation (12,000 g for 10 min), the pellets were boiled at 95 °C for 20 min with 5 × sodium dodecyl sulphate-polyacrylamide gel electrophoresis (SDS-PAGE) loading buffer prior to Western blot assay. (E) A mimic diagram that DNQ-L probe isolated the Keap1 protein from the cell lysates. (F) DNQ-L probe failed to activate Keap1/Nrf2 signal pathway in the presence of NAC. BV2 cells were treated with DNQ-L probe in the presence or absence of NAC for 6 h, then the protein expression in cells was analyzed by Western blot. HO-1: heme oxygenase 1.

along with either WT Flag-Keap1 or Flag-Keap1-Cys489 mutant plasmids. The cells were then treated with DNQ (1  $\mu$ M) for 12 h after 24 h of transfection. The Keap1-Nrf2 complex was identified in the immunoprecipitants using anti-Myc magnetic beads and protein A/G PLUS-agarose. Fig. 9A demonstrated that DNQ effectively disrupted the Keap1-Nrf2 interaction in the WT Keap1 group. However, in the Keap1-Cys489 mutant group, the Keap1-Nrf2 complex was still detected. The results obtained showed that the modification of Keap1-Cys489 by DNQ played a crucial role in initiating the dissociation of the Keap1-Nrf2 complex.

Among the currently proposed patterns associated with the activation of Keap1-Nrf2, one is the Keap1-ubiquitination-mediated Keap1 degradation and Nrf2 release [3]. In this pattern, activators could cause a switch in ubiquitination from Nrf2 to Keap1, which results in the degradation of Keap1 and stabilization of Nrf2. As DNQ was detected to trigger the decrease of Keap1 and increase of Nrf2 in Figs. 4D, 4E, 5C, and 5E, we attempted to examine whether DNQ affected the modulation of Nrf2 ubiquitination and Keap1 ubiquitination. Fig. 9B demonstrated that DNQ dose-dependently increased the Keap1 ubiquitination while suppressed Nrf2 ubiquitination in RAW264.7 cells.

Additionally, the impact of DNQ on Keap1 ubiquitination was further investigated in HEK293T cells. The cells were transfected with Myc3-Nrf2 and mRFP-Ub plasmids along with either WT Flag-Keap1 or Flag-Keap1-Cys489 mutant plasmids. The occurrence of ubiquitination was evaluated by determining the immunoprecipitated Nrf2 or Keap1 after treatment with DNQ (1  $\mu$ M) for 12 h and MG132 (5  $\mu$ M) for an additional 4 h. The result of this assessment

was illustrated in Fig. 9C. The WT Flag-Keap1 group showed an increase in Keap1 ubiquitination and a decrease in Nrf2 ubiquitination upon DNQ induction. However, this effect was not observed in HEK293T cells transfected with the Flag-Keap1-Cys489 mutant. The results indicated that DNQ-mediated alkylation of Keap1-Cys489 triggered the degradation of Keap1 by driving Keap1-ubiquitination.

#### 4. Discussion

DNQ is a natural small molecule initially isolated from south China sea and has been productively biosynthesized utilizing an ocean aerobic actinomycete called *Pseudonocardia antitumoralis* sp. nov [14,15]. In this study, it was discovered that DNQ has remarkable *in vitro* anti-inflammatory properties, even at nanomolar concentrations (Fig. 1), and one-tenth dose of DNQ could exert a comparable inflammation-suppression effect to the positive drug (dimethyl fumarate) in LPS-induced acute inflammatory mice (Fig. 2). Inspired by the previous report [13], we demonstrated that DNQ upregulated HO-1 expression and inhibited inflammation through  $\alpha$ ,  $\beta$ -unsaturated amides moieties such an active group which could be inactivated through the reaction with NAC (Fig. 3).

HO-1, one of the downstream proteins in Keap1/Nrf2 signal pathway, has been widely reported to be an antioxidant and anti-inflammatory marker [33]. Dimethyl fumarate (containing two electrophilic  $\alpha$ ,  $\beta$ -unsaturated carbonyls group in chemical structure) had been approved by US FDA in treating inflammatory disease (Multiple Sclerosis) as a Nrf2 activator [36–38]. 4-octyl

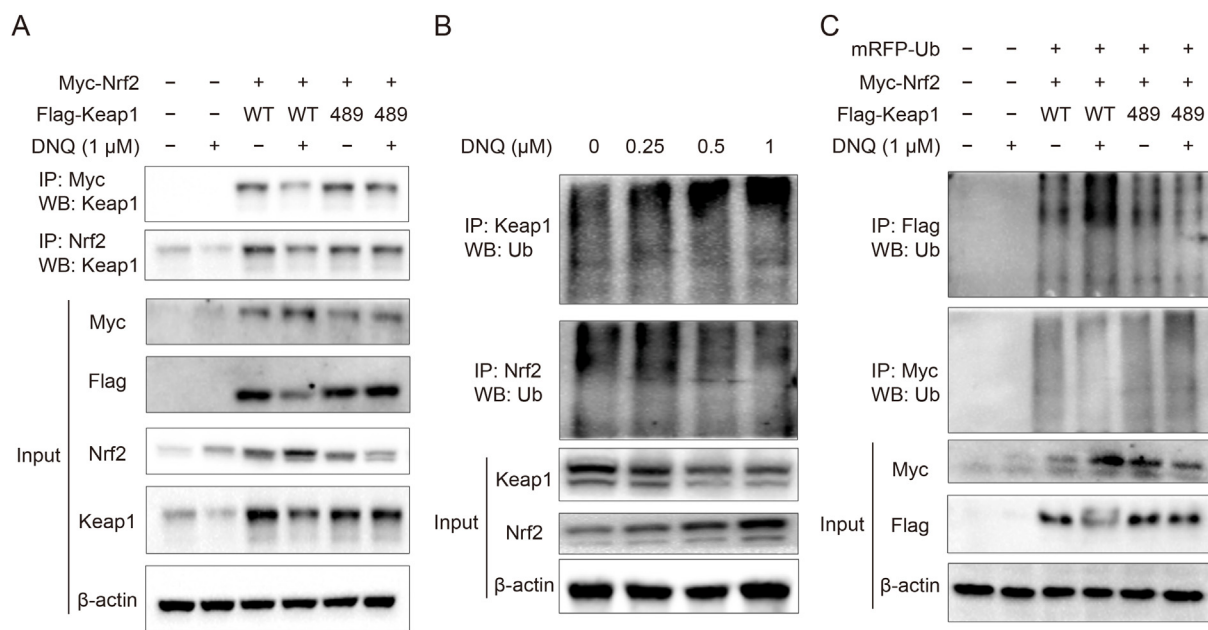


**Fig. 9.** Deoxyneboquinone (DNQ)-mediated alkylation of Kelch-like ECH-associated protein 1 (Keap1)-Cys489 triggered the dissociation of Keap1-nuclear factor erythroid 2-related factor 2 (Nrf2) complex and the degradation of Keap1 by driving Keap1-ubiquitination. (A) DNQ failed to trigger the dissociation of Keap1-Nrf2 complex in the Keap1-Cys489 mutant HEK293T cells. HEK293T cells were seeded in 100 mm culture dish and transfected with Myc-Nrf2 plasmid together with wild type (WT) Flag-Keap1 or Flag-Keap1-C489A plasmid for 24 h and then sub-cultured into two dishes. The sub-cultured cells were treated in the presence or absence of DNQ for 12 h, then total protein expression (Input) in the cell lysates was measured with the anti-Nrf2, anti-Keap1, anti-Myc and anti-Flag antibodies by immunoblot (IB). The Keap1 proteins associated with Nrf2 were detected with an anti-Keap1 antibody after being immunoprecipitated with anti-Myc magnetic beads (IP: Myc) or protein A/G PLUS-agarose (IP: Nrf2). (B) DNQ induced the ubiquitination of Keap1 but decreased the ubiquitination of Nrf2. RAW264.7 cells were treated with DNQ (0, 0.25, 0.5 or 1  $\mu$ M) for 12 h following treatment with 10 mM MG132 for 5 h. Cells were harvested in reduced buffer (containing 2% sodium dodecyl sulphate (SDS), 150 mM NaCl, 10 mM Tris-HCl pH 8.0, and 1 mM dithiothreitol (DTT)) then immediately boiled and diluted five-fold in buffer without SDS. The total protein of Nrf2 and Keap1 (Input) in the cell lysates was detected with anti-Nrf2 and anti-Keap1 antibodies. The ubiquitination levels of Nrf2 and Keap1 in the immunoprecipitants by protein A/G PLUS-agarose (IP: Nrf2, Keap1) were analyzed through IB with an antibody against the ubiquitin. (C) DNQ failed to trigger the ubiquitination of Keap1 in the Keap1-C489 mutant HEK293T cells. HEK293T cells were transfected with Myc3-Nrf2 and mRFP-Ub plasmids together with WT-Flag-Keap1 or Flag-Keap1-C489 mutant plasmid for 24 h and treated with 1  $\mu$ M DNQ for 6 h, following treatment with 10 mM MG132 for 5 h. Cells were harvested in reduced buffer then immediately boiled and diluted five-fold in buffer without SDS. The total protein (Input) of Myc and Flag in the cell lysates were detected with anti-Myc and anti-Flag antibodies, and the ubiquitination levels of Myc-Nrf2 and Flag-Keap1 in the immunoprecipitants by anti-Myc or anti-Flag magnetic beads were evaluated using the anti-Ub antibody with IB.

itaconate (with an electrophilic  $\alpha$ ,  $\beta$ -unsaturated carbonyl group in chemical structure) has been reported to limit inflammation through activating Nrf2 via alkylation of Keap1 [11]. Given a similar structure ( $\alpha$ ,  $\beta$ -unsaturated amide) included in DNQ, we hypothesized that DNQ could activate HO-1 by directly regulating Keap1/Nrf2 signal pathway. Confirmed by *in vitro* and *in vivo* experiments, DNQ was detected to activate Nrf2 and Nrf2-mediated anti-inflammatory/antioxidant genes and proteins (Figs. 4 and 5). Furthermore, the anti-inflammatory effects of DNQ were detected to almost disappear after knocking down the Nrf2, or partially disappear after knocking down the HO-1 (Fig. 6). The results demonstrated that DNQ indeed initiate the anti-inflammatory effects through activation of Nrf2.

Subsequently, we “Fish hooked” the Keap1 from cell lysates with a DNQ-L probe which was synthesized by introducing a minimalist linker [39] in N-9 of DNQ (Fig. 7), and further demonstrated the direct binding of DNQ to four cysteine residues (Cys257, Cys288, Cys297 and Cys489) on Keap1 (Fig. S8). Importantly, Cys489 was identified as the crucial site among the four cysteine residues for DNQ to activate Nrf2 and produce anti-inflammatory effects (Fig. 8). Thereafter, our study showed that the alkylation of Keap1-Cys489 by DNQ resulted in the dissociation of the Keap1-Nrf2 complex and degradation of Keap1 through Keap1-ubiquitination (Fig. 9). These findings suggested the potential activation mechanisms of DNQ on Keap1/Nrf2 signal pathway after targeting Cys489 on Keap1. In accordance with the proposed mechanism of Nrf2 activation by Hong et al. [40], our results suggested the site-specific modification of Keap1 by electrophiles switched ubiquitin targeting from Nrf2 to Keap1, and this target switching mechanism drove Nrf2 activation.

Currently, most pharmacologists reported the activation of electrophiles to Nrf2 by disassociating the Keap1-Nrf2 complex and inhibiting Nrf2-ubiquitination [35,41,42]. However, only a few reports have mentioned the role of Keap1-ubiquitination in Nrf2 activation [40]. This study investigated and demonstrated, for the first time, the alkylation of Keap1-Kleeh domain by electrophile (DNQ) triggered the Keap1-ubiquitination in Nrf2 activation. The varying patterns of Nrf2 activation among electrophiles highlight the significance of the distinct chemical structures in electrophile modifiers, rather than solely relying on the thiol reactivity in Keap1. Not all electrophiles that modify Keap1 could induce Nrf2, and not all modifications made to Keap1 could activate Nrf2 [34]. In this study, we confirmed the important role of DNQ-mediated alkylation/ubiquitination of Keap1 via targeting Cys489 on Nrf2 activation and inflammation inhibition. Together with the previous report by Cheng et al. [35], it is suggested that small molecules, targeting Keap1-Kelch domain which directly associated with Nrf2 (Fig. S1C), could be high potential in activating Nrf2 and treating diseases.

## 5. Conclusions

In summary, the current study identified that DNQ significantly reversed the inflammatory response through activating Nrf2 signal pathway via alkylation/ubiquitination at Cys489 amino residual of Keap1-Kelch domain. Moreover, the  $\alpha$ ,  $\beta$ -unsaturated amides moieties were demonstrated to be a crucial structure in DNQ that is specific to Cys489. The provided data suggested the potential values of targeting Cys489 on Keap1 by DNQ-like small molecules for inflammatory therapies.

## CRedit author statement

**Ke-Gang Linghu:** Conceptualization, Data curation, Formal analysis, Funding acquisition, Investigation, Methodology, Visualization, Writing - original draft preparation, Reviewing and Editing;

**Tian Zhang:** Conceptualization, Investigation, Methodology, Writing - Reviewing and Editing; **Guang-Tao Zhang:** Investigation, Methodology; **Peng Lv:** Methodology, Software; **Wen-Jun Zhang:** Methodology, Validation; **Guan-Ding Zhao:** Investigation, Methodology; **Shi-Hang Xiong:** Investigation; **Qiu-Shuo Ma:** Investigation; **Ming-Ming Zhao:** Investigation, Methodology; **Meiwan Chen:** Methodology; **Yuan-Jia Hu:** Methodology; **Chang-Sheng Zhang:** Funding acquisition, Resources, Supervision; **Hua Yu:** Conceptualization, Funding acquisition, Project administration, Resources, Supervision, Writing - Reviewing and Editing.

## Declaration of competing interest

The authors declare that there are no conflicts of interest.

## Acknowledgments

This study was supported by the Science and Technology Development Fund, Macao SAR (Grant Nos.: No.0159/2020/A3, No.0058/2020/AMJ, No.0096/2019/A2 and SKL-QRCM(UM)-2023-2025), the Research Committee of the University of Macau (Grant No.: MYRG2022-00189-ICMS), the Guangdong Provincial Special Fund for Marine Economic Development Project (Project No.: GDNRC[2021]48), National Natural Science Foundation of China (Grant No.: 82260801), and K.C. Wong Education Foundation (Grant No.: GJTD-2020-12). We greatly appreciate Ms. Parsa Dar for her language help.

## Appendix A. Supplementary data

Supplementary data to this article can be found online at <https://doi.org/10.1016/j.jpha.2023.07.009>.

## References

- [1] A.M. Mahmoud, F.L. Wilkinson, M.A. Sandhu, et al., The interplay of oxidative stress and inflammation: Mechanistic insights and therapeutic potential of antioxidants, *Oxid. Med. Cell. Longev.* 2021 (2021) 1–4.
- [2] E.J. Ramos-González, O.K. Bitzer-Quintero, G. Ortiz, et al., Relationship between inflammation and oxidative stress and its effect on multiple sclerosis, *Neurologia* (2021).
- [3] L. Baird, A.T. Dinkova-Kostova, The cytoprotective role of the Keap1-Nrf2 pathway, *Arch. Toxicol.* 85 (2011) 241–272.
- [4] T.W. Kensler, N. Wakabayashi, S. Biswal, Cell survival responses to environmental stresses via the Keap1-Nrf2-ARE pathway, *Annu. Rev. Pharmacol. Toxicol.* 47 (2007) 89–116.
- [5] S. Magesh, Y. Chen, L. Hu, Small molecule modulators of Keap1-Nrf2-ARE pathway as potential preventive and therapeutic agents, *Med. Res. Rev.* 32 (2012) 687–726.
- [6] M. Lu, J. Ji, Z. Jiang, et al., The Keap1-Nrf2-ARE pathway as a potential preventive and therapeutic target: An update, *Med. Res. Rev.* 36 (2016) 924–963.
- [7] A. Cuadrado, A.I. Rojo, G. Wells, et al., Therapeutic targeting of the NRF2 and KEAP1 partnership in chronic diseases, *Nat. Rev. Drug Discov.* 18 (2019) 295–317.
- [8] A.T. Dinkova-Kostova, W.D. Holtzclaw, T.W. Kensler, The role of Keap1 in cellular protective responses, *Chem. Res. Toxicol.* 18 (2005) 1779–1791.
- [9] A.T. Dinkova-Kostova, R.V. Kostov, P. Canning, Keap1, the cysteine-based mammalian intracellular sensor for electrophiles and oxidants, *Arch. Biochem. Biophys.* 617 (2017) 84–93.
- [10] G. Rachakonda, Y. Xiong, K.R. Sekhar, et al., Covalent modification at Cys151 dissociates the electrophile sensor Keap1 from the ubiquitin ligase CUL3, *Chem. Res. Toxicol.* 21 (2008) 705–710.
- [11] E.L. Mills, D.G. Ryan, H.A. Prag, et al., Itaconate is an anti-inflammatory metabolite that activates Nrf2 via alkylation of KEAP1, *Nature* 556 (2018) 113–117.
- [12] K.L. Rinehart Jr, H.B. Renfroe, The structure of nybomycin, *J. Am. Chem. Soc.* 83 (1961) 3729–3731.
- [13] J.S. Bair, R. Palchadhuri, P.J. Hergenrother, Chemistry and biology of deoxy-nyboquinone, a potent inducer of cancer cell death, *J. Am. Chem. Soc.* 132 (2010) 5469–5478.
- [14] S. Li, X. Tian, S. Niu, et al., Pseudonocardins A–C, new diazaanthraquinone derivatives from a deep-sea actinomycete *Pseudonocardia* sp. SCSIO 01299, *Mar. Drugs* 9 (2011) 1428–1439.

- [15] X. Tian, L. Long, S. Li, et al., *Pseudonocardia antitumoralis* sp. nov., a deoxy-nyboquinone-producing actinomycete isolated from a deep-sea sediment, *Int. J. Syst. Evol. Microbiol.* 63 (2013), 1936.
- [16] E.I. Parkinson, P.J. Hergenrother, Deoxynyboquinones as NQO1-Activated Cancer Therapeutics, *Acc. Chem. Res.* 48 (2015) 2715–2723.
- [17] K. Saleem, W.A. Wani, A. Haque, et al., Synthesis, DNA binding, hemolysis assays and anticancer studies of copper (II), nickel (II) and iron (III) complexes of a pyrazoline-based ligand, *Future Med. Chem.* 5 (2013) 135–146.
- [18] I. Ali, W.A. Wani, K. Saleem, et al., Syntheses, DNA binding and anticancer profiles of L-glutamic acid ligand and its copper (II) and ruthenium (III) complexes, *Med. Chem.* 9 (2013) 11–21.
- [19] I. Ali, W.A. Wani, K. Saleem, et al., Anticancer metallodrugs of glutamic acid sulphonamides: in silico, DNA binding, hemolysis and anticancer studies, *RSC Adv.* 4 (2014) 29629–29641.
- [20] I. Ali, M. Suhail, M. Fazil, et al., Anti-cancer and Anti-oxidant Potencies of *Cuscuta reflexa* Roxb. Plant Extracts, *Am. J. Adv. Drug Deliv.* 14 (2019) 92–113.
- [21] I. Ali, M. Alsehli, L. Scotti, et al., Progress in polymeric nano-medicines for theranostic cancer treatment, *Polymers (Basel)* 12 (2020), 598.
- [22] I. Ali, W.A. Wani, A. Haque, et al., Glutamic acid and its derivatives: candidates for rational design of anticancer drugs, *Future Med. Chem.* 5 (2013) 961–978.
- [23] I. Ali, W.A. Wani, K. Saleem, et al., Thalidomide: A Banned Drug Resurged into Future Anticancer Drug, *Curr. Drug Ther.* 7 (2012) 13–23.
- [24] K.-G. Linghu, G.D. Zhao, W. Xiong, et al., Comprehensive comparison on the anti-inflammatory effects of three species of *Sigesbeckia* plants based on NF- $\kappa$ B and MAPKs signal pathways *in vitro*, *J. Ethnopharmacol.* 250 (2020), 112530.
- [25] K.-G. Linghu, Q.S. Ma, G.D. Zhao, et al., Leocarpinolide B attenuates LPS-induced inflammation on RAW264.7 macrophages by mediating NF- $\kappa$ B and Nrf2 pathways, *Eur. J. Pharmacol.* 868 (2020), 172854.
- [26] T. Toyama, Y. Shinkai, T. Kaji, et al., A convenient method to assess chemical modification of protein thiols by electrophilic metals, *J. Toxicol. Sci.* 38 (2013) 477–484.
- [27] K.-G. Linghu, S.H. Xiong, G.D. Zhao, et al., *Sigesbeckia orientalis* L. extract alleviated the collagen type II-induced arthritis through inhibiting multi-target-mediated synovial hyperplasia and inflammation, *Front. Pharmacol.* 11 (2020), 547913.
- [28] A. Paine, B. Eiz-Vesper, R. Blasczyk, et al., Signaling to heme oxygenase-1 and its anti-inflammatory therapeutic potential, *Biochem. Pharmacol.* 80 (2010) 1895–1903.
- [29] S. Ryter, Therapeutic potential of heme oxygenase-1 and carbon monoxide in acute organ injury, critical illness, and inflammatory disorders, *Antioxidants* 9 (2020), 1153.
- [30] J.A. Araujo, M. Zhang, F. Yin, Heme oxygenase-1, oxidation, inflammation, and atherosclerosis, *Front. Pharmacol.* 3 (2012), 119.
- [31] D.E. Stack, J.A. Conrad, B. Mahmud, Structural identification and kinetic analysis of the *in vitro* products formed by reaction of bisphenol A-3, 4-quinone with N-acetylcysteine and glutathione, *Chem. Res. Toxicol.* 31 (2018) 81–87.
- [32] Y. Cheng, J. Rong, Therapeutic potential of heme oxygenase-1/carbon monoxide system against ischemia-reperfusion injury, *Curr. Pharm. Des.* 23 (2017) 3884–3898.
- [33] S. Nishikawa, Y. Inoue, Y. Hori, et al., Anti-inflammatory activity of kurarinone involves induction of HO-1 via the KEAP1/Nrf2 pathway, *Antioxidants* 9 (2020), 842.
- [34] A.L. Eggler, G. Liu, J.M. Pezzuto, et al., Modifying specific cysteines of the electrophile-sensing human Keap1 protein is insufficient to disrupt binding to the Nrf2 domain Neh2, *Proc. Natl. Acad. Sci. USA* 102 (2005) 10070–10075.
- [35] Y. Cheng, L. Cheng, X. Gao, et al., Covalent modification of Keap1 at Cys77 and Cys434 by pubescenoside a suppresses oxidative stress-induced NLRP3 inflammasome activation in myocardial ischemia-reperfusion injury, *Theranostics* 11 (2021) 861–877.
- [36] N. Robledinos-Antón, R. Fernández-Ginés, G. Manda, et al., Activators and inhibitors of NRF2: A review of their potential for clinical development, *Oxid. Med. Cell. Longev.* 2019 (2019) 1–20.
- [37] U. Schulze-Topphoff, M. Varrin-Doyer, K. Pekarek, et al., Dimethyl fumarate treatment induces adaptive and innate immune modulation independent of Nrf2, *Proc. Natl. Acad. Sci. U. S. A.* 113 (2016) 4777–4782.
- [38] E.A. Mills, M.A. Ogrodnik, A. Plave, et al., Emerging understanding of the mechanism of action for dimethyl fumarate in the treatment of multiple sclerosis, *Front. Neurol.* 9 (2018), 5.
- [39] Z. Li, P. Hao, L. Li, et al., Design and synthesis of minimalist terminal alkyne-containing diazirine photo-crosslinkers and their incorporation into kinase inhibitors for cell- and tissue-based proteome profiling, *Angew. Chem.* 125 (2013) 8713–8718.
- [40] F. Hong, K.R. Sekhar, M.L. Freeman, et al., Specific patterns of electrophile adduction trigger Keap1 ubiquitination and Nrf2 activation, *J. Biol. Chem.* 280 (2005) 31768–31775.
- [41] L. Baird, D. Lières, S. Swift, et al., Regulatory flexibility in the Nrf2-mediated stress response is conferred by conformational cycling of the Keap1-Nrf2 protein complex, *PNAS* 110 (2013) 15259–15264.
- [42] Y. Ying, J. Jin, L. Ye, et al., Phloretin prevents diabetic cardiomyopathy by dissociating Keap1/Nrf2 complex and inhibiting oxidative stress, *Front. Endocrinol.* 9 (2018), 774.